

The electric double layer at the interface between a polyelectrolyte gel and salt bath

Matthew G. Hennessy^{*1,2}, Giulia L. Celora², Andreas Münch², Barbara Wagner³, and Sarah L. Waters²

¹*Department of Engineering Mathematics, University of Bristol, University Walk, Bristol, BS8 1TW, United Kingdom*

²*Mathematical Institute, Woodstock Road, University of Oxford, Oxford, OX2 6GG, United Kingdom*

³*Weierstrass Institute, Mohrenstrasse 39, 10117 Berlin, Germany*

January 28, 2022

Abstract

The electric double layer (EDL) that forms at the interface between a polyelectrolyte gel and a salt bath is studied using asymptotic and numerical methods. Specifically, matched asymptotic expansions, based on the smallness of the Debye length relative to the typical gel dimensions, are used to construct solutions of the governing equations and derive electroneutral models with consistent jump conditions across the gel-bath interface. A general approach for solving the equations of incompressible nonlinear elasticity in a curved boundary layer is developed and used to resolve the gel mechanics in the EDL. A critical feature of the model is that it accounts for phase separation within the gel, which gives rise to diffuse interfaces with a characteristic thickness described by the Kuhn length. We show that the solutions of the electroneutral model can only be asymptotically matched to the solutions in the EDL, in general, when the Kuhn length greatly exceeds the Debye length. Conversely, if the Debye length is similar to or larger than the Kuhn length, then the entire gel can self-organise into periodic, electrically charged domains via phase separation. The breakdown of electroneutrality demonstrates that the commonly invoked electroneutral assumption must be used with caution, as it generally only applies when the Debye length is much smaller than the Kuhn length.

1 Introduction

Polyelectrolyte gels are soft, electro-active materials that are used in a wealth of applications including smart materials [6, 23], fuel cells [15], gel diodes [28], regenerative medicine [17], and drug-delivery systems [18]. A polyelectrolyte gel consists of a network of deformable polymers that is swollen with fluid. The polymers carry a fixed electric charge and can therefore electrostatically interact with ions that are dissolved in the imbibing fluid. Typically, polyelectrolyte gels are surrounded by a bath consisting of a salt solution, which allows for solvent and ion exchange across the gel-bath interface until an equilibrium is established. This equilibrium sets the degree of swelling that occurs in the gel and can be controlled through a number of factors such as temperature and electric fields, as well as the pH and salt content in the surrounding

*matthew.hennessy@bristol.ac.uk

bath [1]. Slight alterations in the environmental parameters can trigger enormous changes in the gel volume. In some cases, the volume of the gel will undergo a discontinuous change, a phenomenon that is called a volume phase transition [5, 20]. Environmental stimuli can also induce phase separation, whereby a homogeneous gel spontaneously separates into co-existing phases with different compositions [16, 24]. Phase separation has been proposed as a facile means of self-assembling nanostructures in polyelectrolyte gels [26, 27].

When a polyelectrolyte gel is surrounded by a salt solution, ions from the solution will migrate to the free surface of the gel and form a diffuse layer of electric charge known as the electric double layer (EDL). Generally, the EDL has two components, the Stern layer and the diffuse layer, that collectively act to screen the electric charges on the polymer chains. The thickness of the EDL is described by the Debye length and is often on the order of tens of nanometers. An interesting feature of polyelectrolyte gels is that the EDL is diffuse on both sides of the gel-bath interface due to the mobile ions in the gel migrating to counter the accumulation of charge in the surrounding bath.

Despite the intricate structure of the EDL, it is generally believed to play a passive role in the gel dynamics and is often neglected in studies that aim to construct new models of polyelectrolyte gels [7, 8, 14, 31] or employ existing models to interpret experimental data [13, 21, 30]. The few exceptions include the works by Hong *et al.* [12] and Wang and Hong [25], who compute solutions in the EDL for a limited range of parameters by prescribing an ad-hoc form of the deformation gradient tensor. The motivation for neglecting the EDL stems from the smallness of the Debye length (tens of nanometers) relative to the typical dimensions of a polyelectrolyte gel (microns to centimeters); thus, any impact of the EDL on the gel dynamics is assumed to be confined to an extremely thin region near the free surface.

To ease the computational burden of resolving the thin EDL, it is common to simplify the governing equations by taking the electroneutral limit, in which the ratio of the Debye length to the characteristic gel size is asymptotically set to zero. The name of the electroneutral limit derives from the fact that, to a very good approximation, the gel and the bath are electrically neutral outside of the EDL. Thus, the electroneutral limit involves collapsing the EDL to a region of zero thickness to produce equations that govern electrically neutral materials. Using matched asymptotic expansions, the bulk equations in the electroneutral limit can be supplemented with jump conditions across the EDL to produce the so-called electroneutral model. Although the electroneutral limit is used extensively when modelling polyelectrolyte gels, very little attention is paid to computing the solution in the EDL and checking that it can be asymptotically matched to the solution of the electroneutral model. Moreover, the jump conditions across the EDL are rarely derived despite being highly non-trivial, as demonstrated by the celebrated Helmholtz–Smoluchowski slip condition for ionic solutions in contact with a rigid solid [29]. Mori *et al.* [19] used matched asymptotics to derive an electroneutral model for a polyelectrolyte gel but did not compute solutions to it nor study the EDL in detail.

The aims of this paper are to use matched asymptotic expansions to: (i) revisit the assumption that the EDL plays a passive role in the dynamics of polyelectrolyte gels and (ii) ascertain the validity of the electroneutral limit. In particular, we will compute the electroneutral model and explore when its solutions can be asymptotically matched to the solutions in the EDL. The main result of our work is that asymptotic matching of solutions cannot always be carried out because the EDL can trigger a mode of phase separation that leads to a breakdown of electroneutrality across the entire gel.

Our asymptotic analysis of the EDL builds on that of Yariv [29] by accounting for the electro-chemo-mechanics of the gel, which requires reformulating and solving the equations of three-dimensional nonlinear elasticity in a curved and evolving boundary layer. By using a general form of the deformation gradient tensor in the analysis, we are able to elucidate how

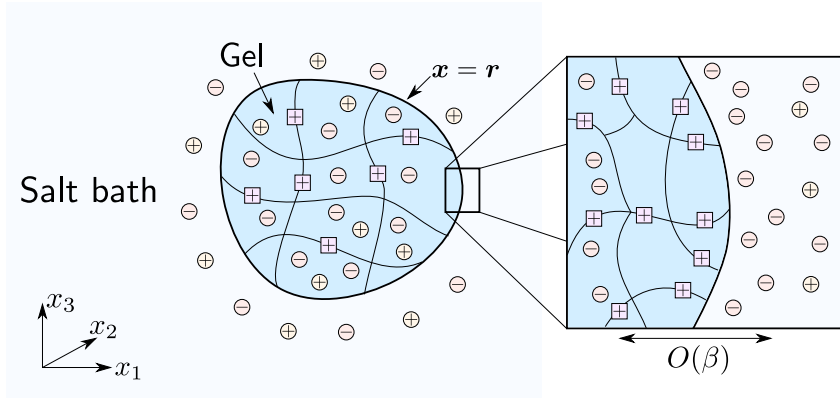


Figure 1: A swollen polyelectrolyte gel surrounded by a bath. The bath consists of a solvent and a dissolved binary salt. The polymers of the gel carry an electric charge, which is assumed to be positive. An electric double layer of thickness $O(\beta)$ forms near the gel-bath interface, located at $\mathbf{x} = \mathbf{r}$, where charge neutrality is violated. The non-dimensional Debye length β is defined in (2.1).

the simplified form proposed by Hong *et al.* [12] and Wang and Hong [25] arises. Another crucial feature of our analysis is that it is based on a phase-field model of a polyelectrolyte gel that can capture phase separation. The use of a phase-field model introduces a new length scale into the problem, the Kuhn length, which characterises the thickness of diffuse interfaces that arise from phase separation. Most models in the literature do not account for phase separation and thus take the Kuhn length to be zero. However, we find that the electroneutral limit is only asymptotically consistent, in general, when the Kuhn length greatly exceeds the Debye length, which prevents the emergence of electrically charged domains in the gel due to phase separation. Thus, we argue that particular care must be taken when applying electroneutral models to experimental data.

The paper is organised as follows. In Sec. 2 the governing equations for a polyelectrolyte gel are presented along with those of the surrounding bath. In Sec. 3 we carry out the asymptotic analysis of the EDL for a general three-dimensional configuration assuming the Kuhn length is much larger than the Debye length. In Sec. 4, we discuss how the analysis differs if the Kuhn length is zero, which is more typical across the literature. The asymptotic framework is then applied to cylindrical polyelectrolyte gels in Sec. 5. The paper concludes in Sec. 6.

2 Mathematical model

We consider a polyelectrolyte gel that is surrounded by a bath, as shown in Fig. 1. The bath consists of a solvent and a dissolved binary salt such as NaCl or CaCl₂. The gel is composed of a crosslinked network of deformable polymers that carry electric charges of the same sign.

Our analysis is based on the thermodynamically consistent model of a polyelectrolyte gel that is surrounded by a viscous bath that has been derived by Celora *et al.* [4]. For brevity, we only present the non-dimensional form of the governing equations in the main text; however, the dimensional model is provided in Appendix A. In the equations below, the subscript m is used to represent quantities associated with the solvent (s), cation ($+$), or the anion ($-$). The subscript n refers to the polymer network. The set $\mathbb{M} = \{s, +, -\}$ contains all of the mobile species that move relative to the polymers. We let $\mathbb{I} = \{+, -\}$ denote the ionic species.

In non-dimensionalising the model, spatial variables are scaled with a characteristic length scale L , which, for example, might represent the size of the gel in its dry or as-prepared states. We choose a time scale associated with solvent diffusion in the gel, $t \sim L^2/D_s^0$ where D_s^0 is

a reference value of the diffusivity. This time scale imparts a velocity scale for each species: $\mathbf{v}_k \sim D_s^0/L$. The chemical potentials of the mobile species are written as $\mu_m = \mu_m^0 + k_B T \mu'_m$, where μ_m^0 is a reference chemical potential, k_B is Boltzmann's constant, and T is the absolute temperature. The diffusives fluxes in the gel and the bath scale like $\mathbf{j}_m \sim D_s^0/(\nu L)$ and $\mathbf{q}_m \sim D_s^0/(\nu L)$, respectively, where ν is a typical molecular volume (assumed to be the same for each mobile species). The electric potential in the bath and the gel is scaled with the thermal voltage, $\Phi \sim k_B T/e$, where e is the elementary charge. Pressure gradients in the gel are assumed to balance the elastic stress, $p \sim G$, where G is the shear modulus of the polymer network. In the bath, pressure gradients are balanced with the Maxwell stress, leading to $p \sim \epsilon^{\text{bath}}(k_B T/e)^2/L^2$, with ϵ^{bath} denoting the electrical permittivity of the bath, which is assumed to be constant.

This scaling introduces four key dimensionless parameters given by

$$\mathcal{G} = \frac{\nu G}{k_B T}, \quad \omega = \frac{L_K}{L}, \quad \beta = \frac{L_D}{L}, \quad \mathcal{N} = \frac{\eta D_s^0}{\epsilon^{\text{bath}}(k_B T/e)^2}, \quad (2.1)$$

where L_K is the Kuhn length, $L_D = (\nu \epsilon^{\text{gel}} k_B T)^{1/2}/e$ is the Debye length, with ϵ^{gel} denoting the electric permittivity of the gel and η the kinematic viscosity of the bath, both of which are assumed to be independent of composition. The parameter \mathcal{G} characterises the energetic cost of elastically deforming the gel relative to the energy that is released upon insertion of a solvent molecule into the polymer network. The parameters ω and β describe the thickness of diffuse internal interfaces and EDL relative to L , respectively. Alternatively, ω can be related to the energetic cost of gradients in the solvent concentration; see Celora *et al.* [4] for details. Finally, \mathcal{N} represents the ratio of the viscous stress to the Maxwell stress in the bath. The magnitudes of these numbers will be estimated in Sec. 2.4.

2.1 Governing equations for the gel

The governing equations for the gel are formulated in terms of Eulerian coordinates $\mathbf{x} = x_i \mathbf{e}_i$ associated with the current state of the system, where \mathbf{e}_i are Cartesian basis vectors. An Eulerian coordinate system enables the equations to be written in a physically intuitive way and it facilitates coupling the gel and bath models via boundary conditions. A detailed account of Eulerian-based hydrogel modelling is provided by Bertrand *et al.* [2]. In Eulerian coordinates, the deformation gradient tensor \mathbf{F} , which describes the distortion of material elements relative to the dry state of the gel, is more readily expressed through its inverse,

$$\mathbf{F}^{-1} = \nabla \mathbf{X}, \quad (2.2)$$

where $\mathbf{X}(\mathbf{x}, t) = X_I \mathbf{E}_I$ are Lagrangian coordinates associated with the reference (dry) state of the gel, \mathbf{E}_I are Cartesian basis vectors in the reference state, and $\nabla = \mathbf{e}_i \partial/\partial x_i$. The adopted conventions for computing derivatives of vectors and tensors are given in Appendix B. The quantity $\mathbf{X}(\mathbf{x}, t)$ provides the Lagrangian coordinates of the material element that is located at the point \mathbf{x} in the current state at time t . The determinant $J = \det \mathbf{F}$ characterises volumetric changes in material elements. Both the polymers and the imbibed salt solution are assumed to be incompressible. As a result, any volumetric change in a solid element must be due to a variation in the amount of fluid contained within that element. This leads to the so-called molecular incompressibility condition

$$J = \left(1 - \sum_{m \in \mathbb{M}} \phi_m \right)^{-1} = \phi_n^{-1}, \quad (2.3)$$

where ϕ_k represent the volume fraction of species k . The volume of fixed charges on the polymers is accounted for in the network fraction ϕ_n . Since J describes the volume of swollen material elements relative to their dry volume, we also refer to it as the swelling ratio. The Lagrangian coordinates \mathbf{X} are convected with material elements and thus satisfy the equation

$$\frac{\partial \mathbf{X}}{\partial t} + \mathbf{v}_n \cdot \nabla \mathbf{X} = 0, \quad (2.4)$$

where \mathbf{v}_n is the velocity of the polymer network. Equation (2.4) can be rearranged to obtain an expression for the velocity \mathbf{v}_n given by

$$\mathbf{v}_n = -\mathbf{F} \frac{\partial \mathbf{X}}{\partial t}, \quad (2.5)$$

where (2.2) has been used to write $\nabla \mathbf{X}$ in terms of \mathbf{F} .

Conservation of polymer, solvent, and ions leads to

$$\frac{\partial \phi_n}{\partial t} + \nabla \cdot (\phi_n \mathbf{v}_n) = 0, \quad (2.6a)$$

$$\frac{\partial \phi_m}{\partial t} + \nabla \cdot (\phi_m \mathbf{v}_n + \mathbf{j}_m) = 0, \quad (2.6b)$$

where $\mathbf{j}_m = \phi_m(\mathbf{v}_m - \mathbf{v}_n)$ is the diffusive flux and $m \in \mathbb{M}$. The volume-averaged mixture velocity in the gel, \mathbf{v} , is defined as, and satisfies,

$$\mathbf{v} \equiv \phi_n \mathbf{v}_n + \sum_{m \in \mathbb{M}} \phi_m \mathbf{v}_m = \mathbf{v}_n + \sum_{m \in \mathbb{M}} \mathbf{j}_m. \quad (2.7)$$

Diffusive transport of solvent and ions is described by a Stefan–Maxwell model. The fluxes are thus given by

$$\mathbf{j}_s = -\mathcal{D}_s(J) \sum_{m \in \mathbb{M}} \phi_m \nabla \mu_m, \quad (2.8a)$$

$$\mathbf{j}_\pm = -\mathcal{D}_\pm \phi_\pm \nabla \mu_\pm + \frac{\phi_\pm}{\phi_s} \mathbf{j}_s, \quad (2.8b)$$

where $\mathcal{D}_s(J) = D_s(J)/D_s^0$ and $\mathcal{D}_\pm = D_\pm/D_s^0$. The dimensional parameters D_s and D_\pm denote the solvent diffusivity relative to the polymer network and the ionic diffusivity relative to a pure solvent bath, respectively. The dependence of \mathcal{D}_s on J reflects the change in diffusivity (or permeability) that occurs as the polymer network is deformed [2]. The chemical potentials can be written as

$$\mu_s = \Pi_s + \mathcal{G}p - \omega^2 \nabla^2 \phi_s, \quad (2.9a)$$

$$\mu_\pm = \Pi_\pm + \mathcal{G}p + z_\pm \Phi, \quad (2.9b)$$

where z_\pm is the valence of the ions and Π_m are osmotic pressures defined as

$$\Pi_s = \log \phi_s + \chi J^{-1}(1 - \phi_s) + J^{-1}, \quad (2.10a)$$

$$\Pi_\pm = \log \phi_\pm + J^{-1}(1 - \chi \phi_s). \quad (2.10b)$$

Here, χ is the Flory interaction parameter, which describes (unfavourable) enthalpic interactions between the solvent molecules and the polymers. The electric potential satisfies

$$-\beta^2 \nabla^2 \Phi = z_+ \phi_+ + z_- \phi_- + z_f \phi_f, \quad (2.11)$$

where ϕ_f represents the volume fraction of fixed charges on the polymer network and z_f denotes the valence of these charges. The nominal volume fraction of fixed charges is $\varphi_f = \phi_f J$. We will focus on cationic gels with positive fixed charges, $z_f > 0$.

The conservation of linear momentum in the gel leads to

$$\nabla \cdot \mathbf{T} = \mathbf{0}, \quad (2.12)$$

where \mathbf{T} is the Cauchy stress tensor, which can be decomposed according to

$$\mathbf{T} = \mathbf{T}_e + \mathbf{T}_K + \mathbf{T}_M - p\mathbf{I}. \quad (2.13a)$$

The first contribution, \mathbf{T}_e , represents the elastic stress tensor and is calculated by assuming the polymer network behaves as a neo-Hookean material. This leads to

$$\mathbf{T}_e = J^{-1}(\mathbf{B} - \mathbf{I}), \quad (2.13b)$$

where $\mathbf{B} = \mathbf{F}\mathbf{F}^T$ is the left Cauchy–Green deformation tensor. The second and third contributions, \mathbf{T}_K and \mathbf{T}_M , correspond to the Korteweg and Maxwell stress tensors, respectively, which capture the force generated within the bulk of the gel due to internal interfaces and electric fields. These tensors can be written as

$$\mathbf{T}_K = \mathcal{G}^{-1}\omega^2 \left[\left(\frac{1}{2} |\nabla\phi_s|^2 + \phi_s \nabla^2 \phi_s \right) \mathbf{I} - \nabla\phi_s \otimes \nabla\phi_s \right], \quad (2.13c)$$

$$\mathbf{T}_M = \mathcal{G}^{-1}\beta^2 \left(\nabla\Phi \otimes \nabla\Phi - \frac{1}{2} |\nabla\Phi|^2 \mathbf{I} \right). \quad (2.13d)$$

The final contribution to the Cauchy stress tensor represents an isotropic stress induced by the fluid pressure.

2.2 Governing equations for the bath

Conservation of solvent and ions in the bath is given by

$$\frac{\partial\phi_m}{\partial t} + \nabla \cdot (\phi_m \mathbf{v} + \mathbf{q}_m) = 0, \quad (2.14)$$

where $m \in \mathbb{M}$, \mathbf{v} is the mixture velocity

$$\mathbf{v} = \sum_{m \in \mathbb{M}} \phi_m \mathbf{v}_m, \quad (2.15)$$

and $\mathbf{q}_m = \phi_m(\mathbf{v}_m - \mathbf{v})$ are the diffusive fluxes. Unlike the gel, the diffusive fluxes in the bath are defined relative to the mixture velocity. The bath is assumed to be free of voids and incompressible, which leads to the following conditions:

$$\sum_{m \in \mathbb{M}} \phi_m = 1, \quad \nabla \cdot \mathbf{v} = 0. \quad (2.16)$$

The diffusive fluxes in the bath are also described using a Stefan–Maxwell model and given by

$$\mathbf{q}_\pm = -\mathcal{D}_\pm \phi_\pm \left(\nabla\mu_\pm - \sum_{m \in \mathbb{M}} \phi_m \nabla\mu_m \right) + \frac{\phi_\pm}{\phi_s} \mathbf{q}_s, \quad (2.17a)$$

$$\mathbf{q}_s = -\mathbf{q}_+ - \mathbf{q}_-. \quad (2.17b)$$

The chemical potentials of the solvent and ions are

$$\mu_s = \log \phi_s + \epsilon_r \beta^2 p, \quad (2.18a)$$

$$\mu_{\pm} = \log \phi_{\pm} + \epsilon_r \beta^2 p + z_{\pm} \Phi, \quad (2.18b)$$

where $\epsilon_r = \epsilon^{\text{bath}}/\epsilon^{\text{gel}}$. The electric potential satisfies

$$-\epsilon_r \beta^2 \nabla^2 \Phi = z_+ \phi_+ + z_- \phi_-. \quad (2.19)$$

Conservation of linear momentum in the bath implies that

$$\nabla \cdot \mathbf{T} = \mathbf{0}, \quad (2.20)$$

where the Cauchy stress tensor is

$$\mathbf{T} = \mathbf{T}_v + \mathbf{T}_M - p \mathbf{I}. \quad (2.21a)$$

The first component captures the viscous stresses in the bath, which is assumed to be a Newtonian incompressible fluid; thus,

$$\mathbf{T}_v = \mathcal{N}(\nabla \mathbf{v} + \nabla \mathbf{v}^T). \quad (2.21b)$$

The Maxwell stress tensor for the bath reads

$$\mathbf{T}_M = \nabla \Phi \otimes \nabla \Phi - \frac{1}{2} |\nabla \Phi|^2 \mathbf{I}. \quad (2.21c)$$

By combining (2.20)–(2.21), we can write the stress balance in non-conservative form,

$$\nabla \cdot \mathbf{T}_v + \nabla^2 \Phi \nabla \Phi = \nabla p, \quad (2.22)$$

which will be advantageous for the asymptotic analysis of the double layer.

2.3 Boundary conditions at the gel-bath interface

In the current configuration, the gel-bath interface is defined by the surface $\mathbf{x} = \mathbf{r}(s_1, s_2, t)$, which is parametrised by s_1 and s_2 . The tangent vectors to the interface are defined as $\mathbf{t}_\alpha = \partial \mathbf{r} / \partial s_\alpha$, $\alpha = 1, 2$. The normal vector to the interface is denoted by $\mathbf{n} = (\mathbf{t}_1 \times \mathbf{t}_2) / |\mathbf{t}_1 \times \mathbf{t}_2|$ and assumed to point from the gel into the bath. The normal velocity of the interface is written as V_n . We use the notation $\mathbf{x} \rightarrow \mathbf{r}^\pm$ to denote approaching the interface from the interior of the bath (+) and gel (-).

The kinematic boundary condition is imposed on the polymer network

$$[\mathbf{v}_n \cdot \mathbf{n} - V_n]_{\mathbf{x}=\mathbf{r}^-} = 0. \quad (2.23)$$

Conservation of solvent and ions across the moving boundary of the gel implies that

$$[\mathbf{j}_m \cdot \mathbf{n}]_{\mathbf{x}=\mathbf{r}^-} = A_m = [\mathbf{q}_m \cdot \mathbf{n} + \phi_m (\mathbf{v}_m \cdot \mathbf{n} - V_n)]_{\mathbf{x}=\mathbf{r}^+}, \quad (2.24)$$

where the A_m are introduced to facilitate the asymptotic matching in Sec. 3. By summing (2.24) over $m \in \mathbb{M}$ and using (2.7) and (2.23), we find that the normal component of the mixture velocity is continuous at the interface,

$$[\mathbf{v} \cdot \mathbf{n}]_{\mathbf{x}=\mathbf{r}^-} = [\mathbf{v} \cdot \mathbf{n}]_{\mathbf{x}=\mathbf{r}^+}, \quad (2.25)$$

which is a reflection of the conservation of total mass.

Continuity of the chemical potential across the interface leads to

$$\mu_m|_{\mathbf{x}=\mathbf{r}^-} = M_m = \mu_m|_{\mathbf{x}=\mathbf{r}^+}. \quad (2.26)$$

Due to the non-local term in the solvent chemical potential (2.9a), an additional boundary condition on the solvent fraction in the gel is required. We impose the variational condition

$$[\nabla\phi_s \cdot \mathbf{n}]_{\mathbf{x}=\mathbf{r}^-} = 0. \quad (2.27)$$

From a physical point of view, this condition implies that the solvent does not preferentially wet or dewet the interface, both of which would lead to a localised gradient in the solvent composition.

After non-dimensionalisation, momentum conservation at the interface leads to

$$[\mathcal{G}\mathbf{T} \cdot \mathbf{n}]_{\mathbf{x}=\mathbf{r}^-} = [\epsilon_r\beta^2\mathbf{T} \cdot \mathbf{n}]_{\mathbf{x}=\mathbf{r}^+}. \quad (2.28)$$

The asymptotic analysis will reveal that the stresses in the bath are $O(\beta^{-1})$ in size. As discussed in Sec. 2.4, typically $\beta \ll \mathcal{G}$ and $\epsilon_r \simeq 1$, meaning that (2.28) can be reduced to a stress-free condition for the gel:

$$[\mathbf{T} \cdot \mathbf{n}]_{\mathbf{x}=\mathbf{r}^-} = \mathbf{0}. \quad (2.29)$$

The final boundary condition that must be imposed on the mechanical problem is a form of slip condition. Here we simply impose continuity of the tangential components of the mixture velocity:

$$[\mathbf{v} \cdot \mathbf{t}_\alpha]_{\mathbf{x}=\mathbf{r}^-} = U_\alpha = [\mathbf{v} \cdot \mathbf{t}_\alpha]_{\mathbf{x}=\mathbf{r}^+}. \quad (2.30)$$

However, this is just one option of several possible consistent conditions. For instance, Mori *et al.* [19] opted for a Navier slip condition on the solvent velocity in their kinetic model of a polyelectrolyte gel, whereas Feng and Young [10] used thermodynamics to derive two different slip conditions for non-ionic gels. The choice of slip condition will not have a significant impact on the asymptotic analysis.

We assume there are no surface charges on the interface and therefore impose continuity of the electric potential and electric displacement:

$$\Phi|_{\mathbf{x}=\mathbf{r}^-} = \Phi|_{\mathbf{x}=\mathbf{r}^+}, \quad (2.31a)$$

$$[\nabla\Phi \cdot \mathbf{n}]_{\mathbf{x}=\mathbf{r}^-} = [\epsilon_r\nabla\Phi \cdot \mathbf{n}]_{\mathbf{x}=\mathbf{r}^+}. \quad (2.31b)$$

2.4 Parameter estimation

We assume that the molecular volume of solvent and ions is $\nu \sim 10^{-28} \text{ m}^3$ [30], the system is held at a temperature of $T = 300 \text{ K}$, and the gels have a length scale of $L \sim 1 \text{ cm}$. Horkay *et al.* [13] measured the shear moduli of polyelectrolyte gels to be around $G \sim 10 \text{ kPa}$, which leads to $\mathcal{G} \sim 10^{-4}$. Yu *et al.* [30] reported values of $\mathcal{G} \sim 10^{-3}$.

We assume that the electrical permittivity of the gel and the bath are approximately the same as water due to the ions being dilute. Thus, we set $\epsilon^{\text{gel}} \simeq \epsilon^{\text{bath}} \simeq 80\epsilon_0$, where ϵ_0 is the permittivity of free space. Hence, $\epsilon_r = \epsilon^{\text{gel}}/\epsilon^{\text{bath}} \simeq 1$. The non-dimensional width of the EDL is then $\beta \sim 10^{-8}$, corresponding to a dimensional value of 0.1 nm. However, we will show in Sec. 5 that this value underestimates the width of the EDL computed from the model.

The dimensionless parameter ω is difficult to estimate due to uncertainties in the values of the Kuhn length. Hua *et al.* [14] set $L_K = 0.9$ nm in their modelling study. Similarly, Wu *et al.* [27] take $L_K = 1$ nm. Both values lead to an estimate of $\omega \sim 10^{-7}$. The estimated values of β and ω suggest that the Debye and Kuhn lengths will be comparable.

Drozdov *et al.* [9] report solvent diffusion coefficients ranging from $D_s^0 \sim 10^{-11}$ m²·s⁻¹ to $D_s \sim 10^{-9}$ m²·s⁻¹. In a dilute solution, the ionic diffusivities are on the order of $D_{\pm} \sim 10^{-9}$ m²·s⁻¹ [22]. Thus, we expect \mathcal{D}_{\pm} to range from 1 to 100. Assuming the solvent is water, which has a viscosity $\eta_w \sim 10^{-3}$ Pa·s, and that the concentration of ions in the bath is small compared to the concentration of solvent molecules, i.e. the bath is a dilute solution, then we can approximate the mixture viscosity η with η_w . Hence, we find that \mathcal{N} ranges from 10^{-2} to 1. The (nominal) volume fraction of fixed charges is reported to range from $\varphi_f \sim 10^{-3}$ to $\varphi_f \sim 10^{-1}$ [12, 30]. The Flory interaction parameter χ is generally a function of the gel composition and temperature. However, we treat χ as a constant, which is a common simplification in the literature. Yu *et al.* [30] use constant values of χ that range from 0.1 to 1.6.

3 Asymptotic analysis for large Kuhn lengths

Matched asymptotic expansions in the limit $\beta \rightarrow 0$ will now be used to formulate and, in some cases, solve the governing equations away from and within the EDL at the gel-bath interface. The analysis in this section will focus on the case when the Kuhn length is much larger than the Debye length; thus, we will consider the limit $\beta \rightarrow 0$ with $\beta \ll \omega$. Although our estimates suggests that ω and β are similar in magnitude and hence the limit $\beta \rightarrow 0$ with $\omega = O(\beta)$ may be more physically accurate, we will show that the asymptotic solutions cannot generally be matched in this case. Analysing the case when $\beta \ll \omega$ provides mathematical and physical insights into why the matching fails.

The asymptotic analysis is split into three parts. In Sec. 3.1, we reduce the model in the outer region away from the gel-bath interface and in doing so formulate the bulk equations for the electroneutral model. In Sec. 3.2, we formulate the problem in the inner region near the gel-bath interface to resolve the EDL. Finally, in Sec. 3.3, we derive asymptotically consistent jump conditions across the EDL for the electroneutral model.

3.1 The outer problem

3.1.1 Electroneutral equations for the bath

Taking $\beta \rightarrow 0$ in (2.19) leads to the electroneutrality condition

$$z_+ \phi_+ + z_- \phi_- = 0. \quad (3.1)$$

When (3.1) is combined with the no-void condition (2.16), the volume fractions of solvent ϕ_s and anions ϕ_- can be eliminated from the problem. By manipulating the ion balances in (2.14), we can arrive at

$$\nabla \cdot (z_+ \mathbf{q}_+ + z_- \mathbf{q}_-) = 0, \quad (3.2)$$

which we interpret as an elliptic equation for the electric potential Φ in the bath. The volume fraction of cation evolves according to

$$\frac{\partial \phi_+}{\partial t} + \mathbf{v} \cdot \nabla \phi_+ + \nabla \cdot \mathbf{q}_+ = 0. \quad (3.3)$$

The fluxes in the bath are given by (2.17) and the chemical potentials reduce to

$$\mu_s = \log \phi_s, \quad (3.4a)$$

$$\mu_{\pm} = \log \phi_{\pm} + z_{\pm} \Phi, \quad (3.4b)$$

which show that the contribution from the pressure can be neglected. Finally, the mixture velocity \mathbf{v} satisfies

$$\mathcal{N} \nabla^2 \mathbf{v} + \nabla^2 \Phi \nabla \Phi = \nabla p, \quad (3.5a)$$

$$\nabla \cdot \mathbf{v} = 0, \quad (3.5b)$$

where \mathcal{N} has been assumed to be independent of composition. The form of (3.5a) shows that Maxwell stresses enter the leading-order momentum balance despite the bath being electrically neutral.

3.1.2 Electroneutral equations for the gel

Taking $\beta \rightarrow 0$ in (2.11) leads to the electroneutrality condition in the gel,

$$z_+ \phi_+ + z_- \phi_- = -z_f \phi_f. \quad (3.6)$$

Using $\phi_f = \varphi_f/J$ along with (2.3) in (3.6), the anion fraction ϕ_- can be eliminated from the outer problem. By multiplying the conservation equation for each ion by their respective valence number z_i and adding, we find that

$$\nabla \cdot (z_+ \mathbf{j}_+ + z_- \mathbf{j}_-) = z_f \left(\frac{\partial \phi_f}{\partial t} + \nabla \cdot (\phi_f \mathbf{v}_n) \right) = 0, \quad (3.7)$$

which determines the electric potential Φ in the gel. The second equality is obtained by writing $\phi_f = \varphi_f/J$, assuming that φ_f is uniform in the reference state, and then using the identity [11]

$$\frac{\partial J}{\partial t} + \mathbf{v}_n \cdot \nabla J = J \nabla \cdot \mathbf{v}_n. \quad (3.8)$$

The solvent and cation fractions satisfy the equations

$$\frac{\partial \phi_s}{\partial t} + \nabla \cdot (\phi_s \mathbf{v}_n + \mathbf{j}_s) = 0, \quad (3.9a)$$

$$\frac{\partial \phi_+}{\partial t} + \nabla \cdot (\phi_+ \mathbf{v}_n + \mathbf{j}_+) = 0, \quad (3.9b)$$

where the fluxes and chemical potentials are given by (2.8)–(2.10). The network velocity \mathbf{v}_n is obtained by solving the mechanical problem, which consists of the kinematic relations in (2.2) and (2.5) and the stress balance

$$\nabla \cdot \mathbf{T}_e + \omega^2 \mathcal{G}^{-1} \phi_s \nabla \nabla^2 \phi_s = \nabla p, \quad (3.10)$$

where the elastic stress tensor is given by (2.13b). Contrary to the bath problem, the form of (3.10) shows that the Maxwell stresses do not contribute to the leading-order stress balance in the gel.

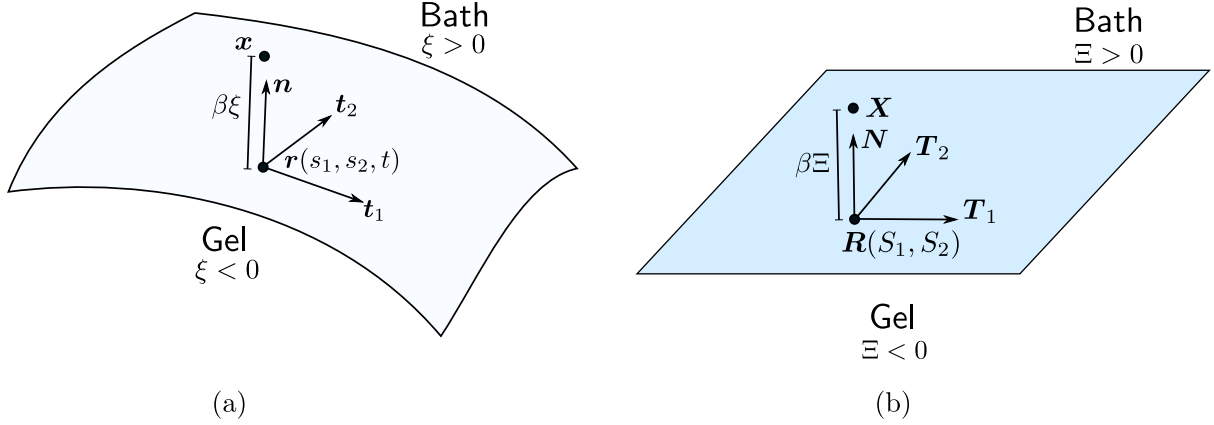


Figure 2: A schematic diagram of the (a) Eulerian and (b) Lagrangian coordinate systems used to formulate the inner problem. The vectors \mathbf{r} and \mathbf{R} , \mathbf{t}_α and \mathbf{T}_α , and \mathbf{n} and \mathbf{N} represent the gel-bath interface, tangent vectors, and unit normal vectors. The interface is parametrised by s_α and S_α , and ξ and Ξ represent coordinates in the normal direction. The gel and bath domains are defined by $\xi, \Xi < 0$ and $\xi, \Xi > 0$, respectively.

3.2 The inner problem

The inner problem is formulated using a surface-fitted coordinate system. This allows a point \mathbf{x} to be represented in terms of its normal distance from the interface and its position along the interface. We thus make the change of variable

$$\mathbf{x} = \mathbf{r}(s_1, s_2, t') + \beta\xi\mathbf{n}(s_1, s_2, t'), \quad t = t', \quad (3.11)$$

where ξ is a coordinate in the normal direction. By convention, the normal vector \mathbf{n} points from the gel to the bath; therefore, $\xi > 0$ corresponds to the regions in the bath whereas $\xi < 0$ corresponds to regions in the gel. An illustration of this coordinate system is provided in Fig. 2 (a). Under this change of variable, the spatial and time derivatives become (see Appendix C for details)

$$\nabla = \beta^{-1}\mathbf{n}\frac{\partial}{\partial\xi} + \nabla_s + O(\beta), \quad (3.12a)$$

$$\nabla^2 = \beta^{-2}\frac{\partial^2}{\partial\xi^2} + 2\beta^{-1}\kappa\frac{\partial}{\partial\xi} + \nabla_s^2 - \xi(\kappa_\alpha\kappa_\alpha)\frac{\partial}{\partial\xi} + O(\beta), \quad (3.12b)$$

$$\frac{\partial}{\partial t} = -\beta^{-1}V_n\frac{\partial}{\partial\xi} + \frac{\partial}{\partial t'} - \frac{\partial\mathbf{r}}{\partial t'} \cdot \nabla_s + O(\beta), \quad (3.12c)$$

where ∇_s and ∇_s^2 are the surface gradient and surface Laplacian, defined in (C.11) and (C.18); κ_1 and κ_2 are the principal curvatures of the interface; and $\kappa = (\kappa_1 + \kappa_2)/2$ is the mean curvature. In deriving (3.12), we have assumed that the non-dimensional curvatures satisfy $\kappa_\alpha = O(1)$ as $\beta \rightarrow 0$, i.e. the dimensional curvature is $O(L^{-1})$ where L is the typical length scale of the gel. In the calculations that follow, the prime on t' will be dropped.

Tildes are used to denote dependent variables in the inner region, which are generally expanded as $\tilde{f} = \tilde{f}^{(0)} + \beta\tilde{f}^{(1)} + O(\beta^2)$, where f is an arbitrary quantity (scalar, vector, tensor). However, additional rescaling is required in some cases; this will be made explicit in the proceeding discussion. Near the interface, the outer solutions for the bath and gel expanded as

$$\lim_{\xi \rightarrow 0^+} f(\mathbf{r} + \beta\xi\mathbf{n}, t) = f^{\text{bath}}(\mathbf{r}, t) + O(\beta), \quad (3.13a)$$

$$\lim_{\xi \rightarrow 0^-} f(\mathbf{r} + \beta\xi\mathbf{n}, t) = f^{\text{gel}}(\mathbf{r}, t) + O(\beta), \quad (3.13b)$$

which will be used for asymptotic matching.

3.2.1 Inner problem for the bath

Mass conservation The $O(\beta^{-1})$ contributions to (2.14) in inner coordinates must satisfy

$$-V_n \frac{\partial \tilde{\phi}_m^{(0)}}{\partial \xi} + \frac{\partial}{\partial \xi} \left(\tilde{\phi}_m^{(0)} \tilde{\mathbf{v}}^{(0)} \cdot \mathbf{n} + \tilde{\mathbf{q}}_m^{(0)} \cdot \mathbf{n} \right) = 0, \quad (3.14)$$

where we have used the fact that \mathbf{n} is independent of ξ . Integrating these equations gives

$$\tilde{\mathbf{q}}_m^{(0)} \cdot \mathbf{n} + \tilde{\phi}_m^{(0)} \left(\tilde{\mathbf{v}}^{(0)} \cdot \mathbf{n} - V_n \right) = A_m(s_1, s_2, t) \quad (3.15)$$

where the integration constant A_m is determined by matching to the outer solution:

$$A_m(s_1, s_2, t) = \mathbf{q}_m^{\text{bath}} \cdot \mathbf{n} + \phi_s^{\text{bath}} (\mathbf{v}_m^{\text{bath}} \cdot \mathbf{n} - V_n). \quad (3.16)$$

The leading-order part of the incompressibility condition for the bath (2.16) is given by

$$\frac{\partial}{\partial \xi} \left(\tilde{\mathbf{v}}^{(0)} \cdot \mathbf{n} \right) = 0. \quad (3.17)$$

Integrating and matching to the outer solution as $\xi \rightarrow \infty$ gives

$$\tilde{\mathbf{v}}^{(0)} \cdot \mathbf{n} = \mathbf{v}^{\text{bath}} \cdot \mathbf{n}. \quad (3.18)$$

Momentum conservation After transforming the Maxwell and viscous stress tensors using (3.12), we anticipate that $\mathbf{T}_M = O(\beta^{-2})$ and $\mathbf{T}_v = O(\beta^{-1})$ as the electric potential $\tilde{\Phi}$ and mixture velocity $\tilde{\mathbf{v}}$ should remain $O(1)$ in size across the EDL. Moreover, we expect that the pressure will scale like the Maxwell stress so that $p = O(\beta^{-2})$. The pressure scaling can be motivated by considering a situation in which the fluid is motionless; in this case, mechanical equilibrium demands that the fluid pressure balances the Maxwell stress, as these are the only two forces at play. Therefore, we write $\mathbf{T}_M = \beta^{-2} \tilde{\mathbf{T}}_M$, $\mathbf{T}_v = \beta^{-1} \tilde{\mathbf{T}}_v$, and $p = \beta^{-2} \tilde{p}$. Consequently, the Cauchy stress tensor must also be scaled as $\mathbf{T} = \beta^{-2} \tilde{\mathbf{T}}$. Expanding $\tilde{\mathbf{T}}$ in powers of β and matching to the far field leads to the stress-free conditions $\tilde{\mathbf{T}}^{(0)} \cdot \mathbf{n} \rightarrow \mathbf{0}$ and $\tilde{\mathbf{T}}^{(1)} \cdot \mathbf{n} \rightarrow \mathbf{0}$ as $\xi \rightarrow \infty$. Taking the normal component of the former and the tangential component of the latter leads to

$$\tilde{p}^{(0)} \rightarrow 0, \quad \xi \rightarrow \infty, \quad (3.19a)$$

$$\mathbf{t}_\alpha \cdot \tilde{\mathbf{T}}_v^{(0)} \cdot \mathbf{n} \rightarrow 0, \quad \xi \rightarrow \infty, \quad (3.19b)$$

where we have exploited the fact that $\partial_\xi \tilde{\Phi}^{(0)} \rightarrow \infty$ as $\xi \rightarrow 0$ to simplify the contributions arising from the Maxwell stresses.

The local form of the stress balance (2.22) is given by

$$\begin{aligned} & \beta \frac{\partial}{\partial \xi} \left(\tilde{\mathbf{T}}_v^{(0)} \cdot \mathbf{n} \right) + \frac{\partial \tilde{\Phi}^{(0)}}{\partial \xi} \frac{\partial^2 \tilde{\Phi}^{(0)}}{\partial \xi^2} \mathbf{n} - 2\beta\kappa \left(\frac{\partial \tilde{\Phi}^{(0)}}{\partial \xi} \right)^2 \mathbf{n} + \beta \frac{\partial \tilde{\Phi}^{(0)}}{\partial \xi} \frac{\partial^2 \tilde{\Phi}^{(1)}}{\partial \xi^2} \mathbf{n} \\ & + \beta \frac{\partial^2 \tilde{\Phi}^{(0)}}{\partial \xi^2} \left(\nabla_s \tilde{\Phi}^{(0)} + \frac{\partial \tilde{\Phi}^{(1)}}{\partial \xi} \mathbf{n} \right) = \frac{\partial \tilde{p}^{(0)}}{\partial \xi} \mathbf{n} + \beta \left(\nabla_s \tilde{p}^{(0)} + \frac{\partial \tilde{p}^{(1)}}{\partial \xi} \mathbf{n} \right) + O(\beta^2). \end{aligned} \quad (3.20)$$

The $O(1)$ contribution can be integrated to obtain a solution for the pressure,

$$\tilde{p}^{(0)} = \mathbf{n} \cdot \tilde{\mathbf{T}}_M^{(0)} \cdot \mathbf{n} = \frac{1}{2} \left(\frac{\partial \tilde{\Phi}^{(0)}}{\partial \xi} \right)^2, \quad (3.21)$$

where the constant of integration has been set to zero using (3.19a). Thus, the pressure in the bath balances the normal component of the Maxwell stresses, as expected. Using the solution for the pressure (3.21) to evaluate the leading-order component of the Cauchy stress tensor reveals that $\tilde{\mathbf{T}}^{(0)} \cdot \mathbf{n} \equiv \mathbf{0}$, implying that the normal stresses in the bath are $O(\beta^{-1})$ in size. This validates reducing the stress-continuity condition (2.28) to the stress-free condition on the gel (2.29).

The $O(\beta)$ problem involves the leading-order contribution to the viscous stress tensor, which is given by

$$\tilde{\mathbf{T}}_v^{(0)} = \mathcal{N} \left(\frac{\partial \tilde{\mathbf{v}}^{(0)}}{\partial \xi} \otimes \mathbf{n} + \mathbf{n} \otimes \frac{\partial \tilde{\mathbf{v}}^{(0)}}{\partial \xi} \right). \quad (3.22)$$

Using the incompressibility condition (3.17), we find that

$$\tilde{\mathbf{T}}_v^{(0)} \cdot \mathbf{n} = \mathcal{N} \frac{\partial \tilde{\mathbf{v}}^{(0)}}{\partial \xi}. \quad (3.23)$$

By using (3.21) and (3.23), the tangential components of the stress balance can be written as

$$\mathcal{N} \frac{\partial^2}{\partial \xi^2} \left(\tilde{\mathbf{v}}^{(0)} \cdot \mathbf{t}_\alpha \right) + \frac{\partial^2 \tilde{\Phi}^{(0)}}{\partial \xi^2} \nabla_s \tilde{\Phi}^{(0)} \cdot \mathbf{t}_\alpha - \frac{\partial \tilde{\Phi}^{(0)}}{\partial \xi} \frac{\partial}{\partial \xi} \left(\nabla_s \tilde{\Phi}^{(0)} \cdot \mathbf{t}_\alpha \right) = 0. \quad (3.24a)$$

This equation has also been derived by Yariv [29]. It can be solved with the boundary conditions

$$\tilde{\mathbf{v}}^{(0)} \cdot \mathbf{t}_\alpha \Big|_{\xi \rightarrow 0^+} = U_\alpha, \quad \frac{\partial}{\partial \xi} \left(\tilde{\mathbf{v}}^{(0)} \cdot \mathbf{t}_\alpha \right) \Big|_{\xi \rightarrow \infty} = 0, \quad (3.24b)$$

where U_α can be computed from the mechanical problem for the gel. The conditions in (3.24b) arise from imposing the slip condition at the gel-bath interface (2.30) and the matching condition (3.19b).

Chemical potentials and fluxes Expanding the chemical potentials gives, to leading order,

$$\tilde{\mu}_s^{(0)} = \log \tilde{\phi}_s^{(0)} + \epsilon_r \tilde{p}^{(0)}, \quad (3.25a)$$

$$\tilde{\mu}_\pm^{(0)} = \log \tilde{\phi}_\pm^{(0)} + \epsilon_r \tilde{p}^{(0)} + z_\pm \tilde{\Phi}^{(0)}. \quad (3.25b)$$

The $O(\beta^{-1})$ contributions to the flux relation (2.17a) gives

$$\frac{\partial \tilde{\mu}_\pm^{(0)}}{\partial \xi} - \sum_{m \in \mathbb{M}} \tilde{\phi}_m^{(0)} \frac{\partial \tilde{\mu}_m^{(0)}}{\partial \xi} = 0. \quad (3.26)$$

The summation in this equation represents a local form of the Gibbs–Duhem relation and is equal to zero. To show this, we first calculate through substitution of (3.25) that

$$\sum_{m \in \mathbb{M}} \tilde{\phi}_m^{(0)} \frac{\partial \tilde{\mu}_m^{(0)}}{\partial \xi} = \epsilon_r \frac{\partial \tilde{p}^{(0)}}{\partial \xi} + \left(z_+ \tilde{\phi}_+^{(0)} + z_- \tilde{\phi}_-^{(0)} \right) \frac{\partial \tilde{\Phi}^{(0)}}{\partial \xi}. \quad (3.27)$$

Inserting the solution for the pressure (3.21) and making use of the leading-order part of the Poisson problem for the voltage,

$$-\epsilon_r \frac{\partial^2 \tilde{\Phi}^{(0)}}{\partial \xi^2} = z_+ \tilde{\phi}_+^{(0)} + z_- \tilde{\phi}_-^{(0)}, \quad (3.28)$$

results in the terms on the right-hand side of (3.27) cancelling out. Therefore, we obtain

$$\sum_{m \in \mathbb{M}} \tilde{\phi}_m^{(0)} \frac{\partial \tilde{\mu}_m^{(0)}}{\partial \xi} = 0. \quad (3.29)$$

From (3.26) and (3.29), we can deduce that the leading-order chemical potentials are uniform across the EDL, giving

$$\log \tilde{\phi}_\pm^{(0)} + \epsilon_r \tilde{p}^{(0)} + z_\pm \tilde{\Phi}^{(0)} = M_\pm(s_1, s_2, t) \quad (3.30a)$$

$$\log \tilde{\phi}_s^{(0)} + \epsilon_r \tilde{p}^{(0)} = M_s(s_1, s_2, t). \quad (3.30b)$$

By imposing the matching conditions $\tilde{\mu}_m^{(0)} \rightarrow \mu_m^{\text{bath}}$, $\tilde{\phi}_m^{(0)} \rightarrow \phi_m^{\text{bath}}$, $\tilde{p}^{(0)} \rightarrow 0$, and $\tilde{\Phi}^{(0)} \rightarrow \Phi^{\text{bath}}$ as $\xi \rightarrow \infty$, we obtain

$$M_\pm(s_1, s_2, t) = \mu_\pm^{\text{bath}} = \log \phi_\pm^{\text{bath}} + z_\pm \Phi^{\text{bath}}, \quad (3.31a)$$

$$M_s(s_1, s_2, t) = \mu_s^{\text{bath}} = \log \phi_s^{\text{bath}}. \quad (3.31b)$$

Equating (3.30a) with (3.31a) provides an expression for the ion fractions in the EDL,

$$\tilde{\phi}_\pm^{(0)} = \phi_\pm^{\text{bath}} \exp \left[z_\pm (\Phi^{\text{bath}} - \tilde{\Phi}^{(0)}) - \epsilon_r \tilde{p}^{(0)} \right]. \quad (3.32)$$

The electrical problem in the bath The leading-order electrical problem is obtained by combining (3.28) with the ionic volume fractions (3.32) to obtain a modified Poisson–Boltzmann equation given by

$$-\epsilon_r \frac{\partial^2 \tilde{\Phi}^{(0)}}{\partial \xi^2} = \exp \left[-(\epsilon_r/2) (\partial \tilde{\Phi}^{(0)} / \partial \xi)^2 \right] \sum_{i \in \mathbb{I}} z_i \phi_i^{\text{bath}} \exp \left(z_i (\Phi^{\text{bath}} - \tilde{\Phi}^{(0)}) \right), \quad (3.33)$$

where we have used (3.21) to eliminate the pressure. The exponential prefactor on the right-hand side of (3.33) is non-standard and results from the ionic chemical potentials depending on the pressure. Equation (3.33) can be integrated once and the conditions $\partial \tilde{\Phi}^{(0)} / \partial \xi \rightarrow 0$ and $\tilde{\Phi}^{(0)} \rightarrow \Phi^{\text{bath}}$ as $\xi \rightarrow \infty$ used to obtain

$$\frac{\partial \tilde{\Phi}^{(0)}}{\partial \xi} = \mp \sqrt{\frac{2}{\epsilon_r} \log \left\{ 1 + \sum_{i \in \mathbb{I}} \phi_i^{\text{bath}} \left[\exp \left(z_i (\Phi^{\text{bath}} - \tilde{\Phi}^{(0)}) \right) - 1 \right] \right\}}. \quad (3.34)$$

The minus sign is taken if $\Phi^{\text{gel}} - \Phi^{\text{bath}} > 0$, which will generally be the case if the fixed charges on the polymer chains are positive, as assumed here.

3.2.2 Inner problem for the gel

Mass conservation Following the same approach as in the bath, the leading-order mass balance for the polymer network leads to

$$-\beta^{-1} V_n \frac{\partial \tilde{\phi}_n^{(0)}}{\partial \xi} + \beta^{-1} \frac{\partial}{\partial \xi} \left(\tilde{\phi}_n^{(0)} \tilde{\mathbf{v}}_n^{(0)} \cdot \mathbf{n} \right) = 0. \quad (3.35)$$

Integrating and imposing the kinematic boundary condition (2.23) at the gel-bath interface ($\xi = 0$) gives

$$\tilde{\mathbf{v}}_n^{(0)} \cdot \mathbf{n} = V_n. \quad (3.36)$$

Similarly, by expressing (2.6b) in inner coordinates, integrating the $O(\beta^{-1})$ contribution, and using (3.36), we find that the diffusive fluxes are uniform and given by

$$\tilde{\mathbf{j}}_m^{(0)} \cdot \mathbf{n} = A_m(s_1, s_2, t) = \mathbf{j}_m^{\text{gel}} \cdot \mathbf{n}. \quad (3.37)$$

where the A_m are the same as in (3.15) and (3.16) due to the boundary conditions (2.24). The second equality in (3.37) comes from matching to the outer solution.

Chemical potentials and fluxes The $O(\beta^{-1})$ contributions to the constitutive relations for the flux (2.8) give

$$\frac{\partial \tilde{\mu}_s^{(0)}}{\partial \xi} = 0, \quad \frac{\partial \tilde{\mu}_\pm^{(0)}}{\partial \xi} = 0, \quad (3.38)$$

implying the chemical potentials in the gel are also constant across the EDL. Thus, we have that

$$\tilde{\mu}_m^{(0)}(\xi, s_1, s_2, t) = M_m(s_1, s_2, t) = \mu_m^{\text{gel}}, \quad (3.39)$$

where M_m are the same as in (3.30). The $O(1)$ contributions to (2.8) provide expressions for the tangential components of the diffusive fluxes,

$$\tilde{\mathbf{j}}_s^{(0)} \cdot \mathbf{t}_\alpha = -\mathcal{D}_s(\tilde{J}^{(0)}) \sum_{m \in \mathbb{M}} \tilde{\phi}_m^{(0)} \nabla_s \mu_m^{\text{gel}} \cdot \mathbf{t}_\alpha, \quad (3.40a)$$

$$\tilde{\mathbf{j}}_\pm^{(0)} \cdot \mathbf{t}_\alpha = -\mathcal{D}_\pm \tilde{\phi}_\pm^{(0)} \nabla_s \mu_\pm^{\text{gel}} \cdot \mathbf{t}_\alpha + \frac{\tilde{\phi}_\pm}{\tilde{\phi}_s^{(0)}} \tilde{\mathbf{j}}_s^{(0)} \cdot \mathbf{t}_\alpha, \quad (3.40b)$$

which will be used in calculating the tangential mixture velocity; see (3.56).

The chemical potential of solvent can be expanded as

$$\begin{aligned} \tilde{\mu}_s^{(0)} = & \tilde{\Pi}_s^{(0)} + \mathcal{G}\tilde{p}^{(0)} - \beta^{-2}\omega^2 \left[\frac{\partial^2}{\partial \xi^2} \left(\tilde{\phi}_s^{(0)} + \beta \tilde{\phi}_s^{(1)} + \beta^2 \tilde{\phi}_s^{(2)} \right) + 2\beta\kappa \frac{\partial}{\partial \xi} \left(\tilde{\phi}_s^{(0)} + \beta \tilde{\phi}_s^{(1)} \right) \right. \\ & \left. + \beta^2 \nabla_s^2 \tilde{\phi}_s^{(0)} - \beta^2 (\kappa_\alpha \kappa_\alpha) \xi \frac{\partial \tilde{\phi}_s^{(0)}}{\partial \xi} \right] + O(\beta). \end{aligned} \quad (3.41)$$

Similarly, the boundary condition at the gel-bath interface (2.27) can be expanded to give $\partial \tilde{\phi}_s^{(n)} / \partial \xi = 0$ at $\xi = 0$ for $n = 0, 1, 2$. The $O(\beta^{-2})$ and $O(\beta^{-1})$ contributions to (3.41) along with the boundary and matching conditions show that the solvent concentration is uniform to leading and next order,

$$\tilde{\phi}_s^{(0)}(\xi, s_1, s_2, t) = \phi_s^{\text{gel}}(s_1, s_2, t), \quad \tilde{\phi}_s^{(1)}(\xi, s_1, s_2, t) = \phi_s^{(1)}(s_1, s_2, t), \quad (3.42)$$

which is a distinguishing feature of the asymptotic limit in which $\beta \rightarrow 0$ with $\omega \gg \beta$. Physically, this result is a consequence of gradients in the solvent concentration having a high energy cost

when the Kuhn length is large. Using (3.42) in (3.41), we find that the solvent chemical potential simplifies to

$$\tilde{\mu}_s^{(0)}(\xi, s_1, s_2, t) = \tilde{\Pi}_s^{(0)} + \mathcal{G}\tilde{p}^{(0)} - \omega^2 \left(\frac{\partial^2 \tilde{\phi}_s^{(2)}}{\partial \xi^2} + \nabla_s^2 \phi_s^{\text{gel}} \right) = M_s(s_1, s_2, t). \quad (3.43)$$

By matching to the outer solution we find that

$$M_s(s_1, s_2, t) = \Pi_s^{\text{gel}} + \mathcal{G}p^{\text{gel}} - \omega^2 \nabla^2 \phi_s^{\text{gel}}. \quad (3.44)$$

The chemical potentials of the ions can be expanded as

$$\tilde{\mu}_{\pm}^{(0)}(s_1, s_2, t) = \log \tilde{\phi}_{\pm}^{(0)} + \frac{1}{\tilde{j}^{(0)}}(1 - \chi \phi_s^{\text{gel}}) + \mathcal{G}\tilde{p}^{(0)} + z_{\pm} \tilde{\Phi}^{(0)} = M_{\pm}(s_1, s_2, t), \quad (3.45)$$

where matching gives

$$M_{\pm}(s_1, s_2, t) = \log \phi_{\pm}^{\text{gel}} + \frac{1}{J^{\text{gel}}}(1 - \chi \phi_s^{\text{gel}}) + \mathcal{G}p^{\text{gel}} + z_{\pm} \Phi^{\text{gel}}. \quad (3.46)$$

By combining (3.45) and (3.46) and using (3.42) we find that

$$\tilde{\phi}_{\pm}^{(0)} = \phi_{\pm}^{\text{gel}} \exp \left[z_{\pm} (\Phi^{\text{gel}} - \tilde{\Phi}^{(0)}) + \mathcal{G}(p^{\text{gel}} - \tilde{p}^{(0)}) + \left(\frac{1}{J^{\text{gel}}} - \frac{1}{\tilde{j}^{(0)}} \right) (1 - \chi \phi_s^{\text{gel}}) \right]. \quad (3.47)$$

Although this appears to be a closed-form expression for the volume fraction of ions, it is important to recall that the Jacobian determinant J also depends on these quantities; see (2.3).

Kinematics Before proceeding with the stress balance in the gel, we derive local forms of the deformation gradient tensor, displacement, and velocity of the polymer network that are valid for arbitrary deformations. In Appendix D, the results are specialised to plane-strain problems.

We first consider the Lagrangian representation of the free surface, which is written as $\mathbf{X} = \mathbf{R}(S_1, S_2)$, where S_1 and S_2 are parameters. The Lagrangian tangent and unit normal vectors are denoted by $\mathbf{T}_{\alpha} = \partial \mathbf{R} / \partial S_{\alpha}$ and \mathbf{N} , respectively, where we adopt the convention that Greek indices are equal to 1 or 2 and the Einstein summation convention for repeated indices. We now write the Lagrangian coordinates \mathbf{X} using an analogous representation as in (3.11) for Eulerian coordinates,

$$\mathbf{X} = \mathbf{R}(S_1, S_2) + \beta \Xi \mathbf{N}(S_1, S_2), \quad (3.48)$$

where Ξ is the Lagrangian counterpart to ξ ; see Fig. 2 for an illustration. Due to our formulation of the governing equations in terms of Eulerian coordinates, we have, in the notation of inner variables, $S_{\alpha} = \tilde{S}_{\alpha}(s_1, s_2, \xi, t)$ and $\Xi = \tilde{\Xi}(s_1, s_2, \xi, t)$. We further impose that $\Xi = 0$ when $\xi = 0$. The deformation gradient tensor can be written as

$$\tilde{\mathbf{F}}^{-1} = \beta^{-1} \frac{\partial \tilde{S}_{\alpha}}{\partial \xi} \mathbf{T}_{\alpha} \otimes \mathbf{n} + \frac{\partial}{\partial \xi} (\tilde{\Xi} \mathbf{N}) \otimes \mathbf{n} + \nabla_s \mathbf{R} + O(\beta). \quad (3.49)$$

As before, we now expand \tilde{S}_{α} , $\tilde{\Xi}$, $\tilde{\mathbf{X}}$, and $\tilde{\mathbf{F}}$ in powers of β . The $O(\beta^{-1})$ components of (3.49) imply that $\tilde{S}_{\alpha}^{(0)}$ are independent of ξ and thus $\tilde{S}_{\alpha}^{(0)} = S_{\alpha}^{\text{gel}}(s_1, s_2, t)$. Using the expression for the surface gradient in (C.11), we can define the (inverse) surface deformation gradient tensor as

$$\tilde{\mathbf{F}}_s^{-1} \equiv \nabla_s \mathbf{R}(S_1^{\text{gel}}, S_2^{\text{gel}}) = g^{\delta\gamma} \frac{\partial S_{\alpha}^{\text{gel}}}{\partial s_{\gamma}} \mathbf{T}_{\alpha} \otimes \mathbf{t}_{\delta}, \quad (3.50)$$

where $g^{\delta\gamma}$ are components of the inverse metric tensor. The tensor $\tilde{\mathbf{F}}_s$ contains information about the stretching of material elements in the tangential directions. The $O(1)$ component of (3.49) can be written as

$$\left(\tilde{\mathbf{F}}^{(0)}\right)^{-1} = \frac{\partial\tilde{\Xi}^{(0)}}{\partial\xi}\mathbf{N} \otimes \mathbf{n} + \frac{\partial\tilde{S}_\alpha^{(1)}}{\partial\xi}\mathbf{T}_\alpha \otimes \mathbf{n} + \tilde{\mathbf{F}}_s^{-1}. \quad (3.51)$$

We will show below that the tangential stress balances in the gel lead to $\partial\tilde{S}_\alpha^{(1)}/\partial\xi = 0$, which allows the deformation gradient tensor to be expressed as

$$\tilde{\mathbf{F}}^{(0)} = \left(\frac{\partial\tilde{\Xi}^{(0)}}{\partial\xi}\right)^{-1} \mathbf{n} \otimes \mathbf{N} + \tilde{\mathbf{F}}_s. \quad (3.52)$$

The deformation gradient tensor used by Hong *et al.* [12, 25] can be obtained from (3.52) by setting $\tilde{\mathbf{F}}_s = \lambda_s(\mathbf{t}_1 \otimes \mathbf{T}_1 + \mathbf{t}_2 \otimes \mathbf{T}_2)$ where λ_s is an imposed stretch along the tangential directions. Taking the determinant of (3.52) leads to

$$\tilde{j}^{(0)} = \left(\frac{\partial\tilde{\Xi}^{(0)}}{\partial\xi}\right)^{-1} \det \tilde{\mathbf{F}}_s, \quad (3.53)$$

which can be equated to (2.3) to eliminate $\tilde{\Xi}^{(0)}$ from the problem. By matching (3.52) to the outer solution for the deformation gradient tensor, we find that

$$\mathbf{t}_\delta \cdot \tilde{\mathbf{F}}_s \cdot \mathbf{T}_\gamma = \mathbf{t}_\delta \cdot \mathbf{F}^{\text{gel}} \cdot \mathbf{T}_\gamma, \quad (3.54)$$

which provides a system of differential equations that can be used to determine S_α^{gel} .

The inner expansion of the velocity of the polymer network can be calculated from (2.5) using the representations for \mathbf{X} and \mathbf{F} given by (3.48) and (3.52). The leading-order contribution can be expressed as

$$\tilde{\mathbf{v}}_n^{(0)} = V_n \mathbf{n} + \mathbf{l}_s \cdot \frac{\partial \mathbf{r}}{\partial t} - \tilde{\mathbf{F}}_s \cdot \left(\mathbf{T}_\alpha \frac{\partial S_\alpha^{\text{gel}}}{\partial t} \right), \quad (3.55)$$

where $\mathbf{l}_s = \tilde{\mathbf{F}}_s \tilde{\mathbf{F}}_s^{-1} = g^{\alpha\nu} \mathbf{t}_\alpha \otimes \mathbf{t}_\nu$ is the surface identity tensor. The tangential components of the mixture velocity can then be evaluated using (2.7) as

$$\tilde{\mathbf{v}}^{(0)} \cdot \mathbf{t}_\nu = \frac{\partial \mathbf{r}}{\partial t} \cdot \mathbf{t}_\nu - \mathbf{t}_\nu \cdot \tilde{\mathbf{F}}_s \cdot \left(\mathbf{T}_\alpha \frac{\partial S_\alpha^{\text{gel}}}{\partial t} \right) + \sum_{m \in \mathbb{M}} \tilde{\mathbf{j}}_m^{(0)} \cdot \mathbf{t}_\nu, \quad (3.56)$$

where the tangential components of the flux are given by (3.40). Taking the limit of (3.56) as $\xi \rightarrow 0^-$ enables the quantity U_α in (3.24b) to be determined.

Momentum conservation The leading-order part of the stress balance in the gel (2.12), expressed in inner coordinates, is

$$\frac{\partial}{\partial \xi} \left(\tilde{\mathbf{T}}^{(0)} \cdot \mathbf{n} \right) = 0. \quad (3.57)$$

Thus, by integrating (3.57) and imposing the simplified boundary condition (2.29), we find that

$$\tilde{\mathbf{T}}^{(0)} \cdot \mathbf{n} = \tilde{\mathbf{T}}_e^{(0)} \cdot \mathbf{n} + \tilde{\mathbf{T}}_M^{(0)} \cdot \mathbf{n} + \tilde{\mathbf{T}}_K^{(0)} \cdot \mathbf{n} - \tilde{p}^{(0)} \mathbf{n} = 0 \quad (3.58)$$

across the EDL. The leading-order elastic, Maxwell, and Korteweg stress tensors are

$$\tilde{\mathbf{T}}_e^{(0)} = \frac{1}{\tilde{J}^{(0)}} \left(\tilde{\mathbf{B}}^{(0)} - \mathbf{I} \right), \quad (3.59a)$$

$$\tilde{\mathbf{T}}_M^{(0)} = \frac{1}{\mathcal{G}} \left(\frac{\partial \tilde{\Phi}^{(0)}}{\partial \xi} \right)^2 \left(\mathbf{n} \otimes \mathbf{n} - \frac{1}{2} \mathbf{I} \right), \quad (3.59b)$$

$$\tilde{\mathbf{T}}_K^{(0)} = \frac{\omega^2}{\mathcal{G}} \left\{ \left[\frac{1}{2} |\nabla_s \phi_s^{\text{gel}}|^2 + \phi_s^{\text{gel}} \left(\frac{\partial^2 \tilde{\phi}_s^{(2)}}{\partial \xi^2} + \nabla_s^2 \phi_s^{\text{gel}} \right) \right] \mathbf{I} - \nabla_s \phi_s^{\text{gel}} \otimes \nabla_s \phi_s^{\text{gel}} \right\}. \quad (3.59c)$$

Since $\mathbf{t}_\gamma \cdot \tilde{\mathbf{T}}_M^{(0)} \cdot \mathbf{n} = 0$ and $\mathbf{t}_\gamma \cdot \tilde{\mathbf{T}}_K^{(0)} \cdot \mathbf{n} = 0$, the tangential component of (3.58) implies that

$$\mathbf{t}_\gamma \cdot \tilde{\mathbf{B}}^{(0)} \cdot \mathbf{n} = 0. \quad (3.60)$$

By inverting (3.51) and calculating $\tilde{\mathbf{B}}^{(0)}$, we find that the tangential stress balances (3.60) imply that $\partial \tilde{S}_\alpha^{(1)} / \partial \xi = 0$, as previously claimed. The normal component of (3.58) implies that

$$\tilde{p}^{(0)} = \mathbf{n} \cdot \left(\tilde{\mathbf{T}}_e^{(0)} + \tilde{\mathbf{T}}_K^{(0)} + \tilde{\mathbf{T}}_M^{(0)} \right) \cdot \mathbf{n}. \quad (3.61)$$

In order to evaluate the Korteweg stresses without explicitly solving for $\tilde{\phi}_s^{(2)}$, the expression for the solvent chemical potential (3.43) can be used in (3.59c) to obtain

$$\mathbf{n} \cdot \tilde{\mathbf{T}}_K^{(0)} \cdot \mathbf{n} = \frac{1}{\mathcal{G}} \left[\frac{\omega^2}{2} |\nabla_s \phi_s^{\text{gel}}|^2 + \phi_s^{\text{gel}} \left(\tilde{\Pi}_s^{(0)} - M_s \right) \right] + \phi_s^{\text{gel}} \tilde{p}^{(0)}. \quad (3.62)$$

where M_s is given by (3.44). Note that setting $\omega = 0$ in (3.62) results in $\mathbf{n} \cdot \tilde{\mathbf{T}}_K^{(0)} \cdot \mathbf{n} = 0$, as expected. This is because $\omega = 0$ leads to $\tilde{\Pi}_s^{(0)} + \mathcal{G} \tilde{p}^{(0)} - M_s = 0$ from (3.43). Substitution of (3.62) into (3.61) gives an algebraic relation for the pressure $\tilde{p}^{(0)}$.

The electrical problem in the gel The leading-order electrical problem in the gel is given by

$$-\frac{\partial^2 \tilde{\Phi}^{(0)}}{\partial \xi^2} = z_+ \tilde{\phi}_+^{(0)} + z_- \tilde{\phi}_-^{(0)} + z_f \tilde{\phi}_f^{(0)}, \quad (3.63)$$

which is coupled to the algebraic equations for the volume fractions of ions (3.47) and the mechanical pressure (3.61). The electrical problems for the bath and gel can be decoupled by combining the first integral for the electric potential in the bath (3.34) with the electrostatic boundary conditions $\tilde{\Phi}^{(0)}(0^-, s_1, s_2, t) = \tilde{\Phi}^{(0)}(0^+, s_1, s_2, t)$ and $\partial_\xi \tilde{\Phi}^{(0)}(0^-, s_1, s_2, t) = \epsilon_r \partial_\xi \tilde{\Phi}^{(0)}(0^+, s_1, s_2, t)$ to obtain

$$\left. \frac{\partial \tilde{\Phi}^{(0)}}{\partial \xi} \right|_{\xi=0^-} = \mp \sqrt{2\epsilon_r \log \left\{ 1 + \sum_{i \in \mathbb{I}} \phi_i^{\text{bath}} \left[\exp \left(z_i (\Phi^{\text{bath}} - \tilde{\Phi}^{(0)}) \right) - 1 \right] \right\}} \Big|_{\xi=0^-}, \quad (3.64a)$$

which acts as a boundary condition for (3.63). The electrical problem in the gel is closed by imposing the matching condition

$$\tilde{\Phi}^{(0)} \rightarrow \Phi^{\text{gel}}, \quad \xi \rightarrow -\infty. \quad (3.64b)$$

3.3 Jump conditions across the gel-bath interface

Asymptotically consistent jump conditions across the EDL for the electroneutral model are derived by connecting the inner and outer solutions in the bath and gel via the boundary conditions the gel-bath interface.

Kinematic conditions By imposing mass conservation at the gel-bath interface (2.24), we can equate (3.16) with (3.37) to obtain

$$\mathbf{j}_m^{\text{gel}} \cdot \mathbf{n} = \mathbf{q}_m^{\text{bath}} \cdot \mathbf{n} + \phi_m^{\text{bath}} (\mathbf{v}^{\text{bath}} \cdot \mathbf{n} - V_n). \quad (3.65)$$

Moreover, by matching (3.36) to the solution as $\xi \rightarrow -\infty$, the outer problem obeys the usual kinematic boundary condition (2.23) on the network

$$\mathbf{v}_n^{\text{gel}} \cdot \mathbf{n} - V_n = 0. \quad (3.66)$$

By summing (3.65) over $m \in \mathbb{M}$, the mixture velocities are found to satisfy

$$\mathbf{v}^{\text{gel}} \cdot \mathbf{n} = \mathbf{v}^{\text{bath}} \cdot \mathbf{n}. \quad (3.67)$$

Assuming the anion fraction is eliminated from the outer problems, then only the jump conditions for the solvent and cation in (3.65) need to be imposed. However, the jump conditions for the ions can be combined to obtain

$$(z_+ \mathbf{j}_+^{\text{gel}} + z_- \mathbf{j}_-^{\text{gel}}) \cdot \mathbf{n} = (z_+ \mathbf{q}_+^{\text{bath}} + z_- \mathbf{q}_-^{\text{bath}}) \cdot \mathbf{n}, \quad (3.68)$$

which provides a condition on the normal derivatives of the electric potential.

Continuity of chemical potentials By combining (2.26) along with (3.31) and (3.39), continuity of chemical potential across the interface is recovered: $\mu_m^{\text{gel}} = \mu_m^{\text{bath}}$. Continuity of the solvent chemical potential means that (3.44) can be equated with (3.31b) to produce

$$\Pi_s^{\text{gel}} + \mathcal{G}p^{\text{gel}} - \omega^2 \nabla^2 \phi_s^{\text{gel}} = \log \phi_s^{\text{bath}}. \quad (3.69)$$

Equating the chemical potentials of the ions, i.e. (3.31a) with (3.46), provides a jump condition for the ionic volume fractions

$$\phi_{\pm}^{\text{gel}} = \phi_{\pm}^{\text{bath}} \exp \left[z_{\pm} (\Phi^{\text{bath}} - \Phi^{\text{gel}}) - \mathcal{G}p^{\text{gel}} - \frac{1}{J^{\text{gel}}} (1 - \chi \phi_s^{\text{gel}}) \right]. \quad (3.70)$$

Using (3.70) in the electroneutrality condition for the gel (3.6) produces a jump condition for the electrical potentials

$$\sum_{i \in \mathbb{I}} z_i \phi_i^{\text{bath}} \exp \left(z_i (\Phi^{\text{bath}} - \Phi^{\text{gel}}) \right) = z_f \phi_f \exp \left[\mathcal{G}p^{\text{gel}} + \frac{1}{J^{\text{gel}}} (1 - \chi \phi_s^{\text{gel}}) \right]. \quad (3.71)$$

These equations are also coupled to the molecular incompressibility condition in the gel (2.3), the no-void condition in the bath (2.16), and the electroneutrality condition in the bath (3.1).

Variational condition Matching the derivatives of the solvent fraction in the gel using (3.42) recovers the variational condition

$$\nabla \phi_s^{\text{gel}} \cdot \mathbf{n} = 0. \quad (3.72)$$

Continuity of stress By matching (3.58) with the outer solution, we obtain stress-free conditions for the gel at the interface:

$$\mathbf{T}^{\text{gel}} \cdot \mathbf{n} = 0. \quad (3.73)$$

Slip condition The final boundary condition for the electroneutral model is a slip condition on the mixture velocity of the bath. This is obtained by solving (3.24), where the value of U_α can be derived from the gel problem (3.56) by taking the limit $\xi \rightarrow 0^-$, and then imposing the matching conditions $\tilde{\mathbf{v}}^{(0)} \cdot \mathbf{t}_\alpha \rightarrow \mathbf{v}^{\text{bath}} \cdot \mathbf{t}_\alpha$ as $\xi \rightarrow \infty$. The final result is a Helmholtz–Smoluchowski slip condition for a deformable porous solid.

4 Asymptotic analysis for Kuhn lengths of zero

The asymptotic analysis of the inner region is slightly different for models that neglect phase separation and set the Kuhn length to zero, $\omega = 0$. From (3.41), the leading-order contribution to the solvent chemical potential μ_s in the EDL now becomes

$$\tilde{\mu}_s^{(0)} = \tilde{\Pi}_s^{(0)} + \mathcal{G}\tilde{p}^{(0)} = \mu_s^{\text{gel}}, \quad (4.1a)$$

which can be interpreted as a nonlinear algebraic equation for $\tilde{\phi}_s^{(0)} = \phi_s^{(0)}(\xi, s_1, s_2, t)$. Importantly, the solvent fraction can now vary across the EDL as a result of the complex interplay between mechanics, electrostatics, and thermodynamics captured by (4.1a). The corresponding ion fractions are given by

$$\tilde{\phi}_\pm^{(0)} = \phi_\pm^{\text{gel}} \exp \left[z_\pm (\Phi^{\text{gel}} - \tilde{\Phi}^{(0)}) + \mathcal{G}(p^{\text{gel}} - \tilde{p}^{(0)}) + \frac{1 - \chi\phi_s^{\text{gel}}}{J^{\text{gel}}} - \frac{1 - \chi\tilde{\phi}_s^{(0)}}{\tilde{J}^{(0)}} \right]. \quad (4.1b)$$

The pressure in the gel across the EDL can be calculated directly from (3.61) after neglecting the Korteweg stresses. The jump conditions across the EDL are the same as those in Sec. 3.3, except the $\nabla^2\phi_s^{\text{gel}}$ term in (3.69) and the variational condition in (3.72) can be dropped.

5 Swelling of a constrained cylinder

We now use our formulation to study the EDL forming in cylindrical polyelectrolyte gels that are in equilibrium with an external bath. Following the experimental setup considered by Horkay *et al.* [13], we assume the gel can freely swell in the radial direction but is confined in the axial direction. We consider axisymmetric equilibrium solutions and let r and R denote the Eulerian and Lagrangian radial coordinates, respectively. The deformation gradient tensor can be written as

$$\mathbf{F} = \lambda_r \mathbf{e}_r \otimes \mathbf{E}_R + \lambda_\theta \mathbf{e}_\theta \otimes \mathbf{E}_\Theta + \lambda_z \mathbf{e}_z \otimes \mathbf{E}_Z, \quad (5.1)$$

where $\lambda_r = (\partial R/\partial r)^{-1}$, $\lambda_\theta = r/R$, and λ_z note the radial, orthonormal, and experimentally controlled axial stretch, respectively. The normal and tangent vectors to the free surface are given by $\mathbf{n} = \mathbf{e}_r$, $\mathbf{N} = \mathbf{E}_R$; $\mathbf{t}_1 = \mathbf{e}_\theta$, $\mathbf{T}_1 = \mathbf{E}_\Theta$; $\mathbf{t}_2 = \mathbf{e}_z$ and $\mathbf{T}_2 = \mathbf{E}_Z$. We choose the non-dimensionalisation such that the radius of the cylinder in the reference configuration is scaled to unity. The radius in the current configuration is denoted by a . We thus have that $R(r=0) = 0$ and $R(r=a) = 1$. We restrict our attention to monovalent salts with $z_\pm = \pm 1$. At equilibrium, the solution to the outer problem for the bath corresponds to a uniform composition and electric potential. Using the electroneutrality and no-void conditions for the bath, we obtain

$\phi_s^{\text{bath}} = 1 - 2\phi_+^{\text{bath}}$. The cation fraction, ϕ_+^{bath} , is treated as a free parameter. The electric potential, Φ^{bath} , is treated as an arbitrary constant, which we assume is non-zero for generality.

In Sec. 5.1, the outer problem in the gel is formulated. This consists of a system of nonlinear algebraic equations for homogeneously swollen states that are in equilibrium with the bath. In Sec. 5.2, the corresponding inner problems are formulated for models in the case $\omega = 0$ and $\omega \gg \beta$. The inner solution is validated against a full numerical solution in Sec. 5.3 and used to explore the structure of the EDL in Sec. 5.4.

5.1 Solution of the outer problem: homogeneous equilibria

At equilibrium, the chemical potentials in the gel must be spatially uniform, leading to $\mu_m = \mu_m^{\text{gel}}$ for $m \in \mathbb{M}$. We assume that the outer solution corresponds to a homogeneously swollen cylindrical gel, in which case $\phi_m = \phi_m^{\text{gel}}$ for $m \in \mathbb{M}$. The deformation gradient tensor is given by

$$\mathbf{F}^{\text{gel}} = (J^{\text{gel}}/\lambda_z)^{1/2} (\mathbf{n} \otimes \mathbf{N} + \mathbf{t}_1 \otimes \mathbf{T}_1) + \lambda_z \mathbf{t}_2 \otimes \mathbf{T}_2. \quad (5.2)$$

Consequently, the radial and orthoradial components of the elastic stress tensor are $\mathbb{T}_{e,\theta\theta} = \mathbb{T}_{e,rr} = \lambda_z^{-1} - (J^{\text{gel}})^{-1}$. The stress balance in the hydrogel reduces to $\partial p / \partial r = 0$. Imposing the matching condition (3.73) reveals that the pressure balances the radial elastic stress, $p^{\text{gel}} = \mathbb{T}_{e,rr}^{\text{gel}}$. The volume fraction of solvent and ions, as well as the electric potential, are determined from the jump conditions

$$\log \phi_s^{\text{gel}} + \frac{1}{J^{\text{gel}}} + \frac{\chi(1 - \phi_s^{\text{gel}})}{J^{\text{gel}}} + \mathcal{G} \left(\frac{1}{\lambda_z} - \frac{1}{J^{\text{gel}}} \right) = \log(1 - 2\phi_+^{\text{bath}}), \quad (5.3a)$$

$$\phi_{\pm}^{\text{gel}} = \phi_+^{\text{bath}} \exp \left[\pm (\Phi^{\text{bath}} - \Phi^{\text{gel}}) - \mathcal{G} \left(\frac{1}{\lambda_z} - \frac{1}{J^{\text{gel}}} \right) - \frac{1}{J^{\text{gel}}} (1 - \chi \phi_s^{\text{gel}}) \right], \quad (5.3b)$$

$$2\phi_+^{\text{bath}} \sinh(\Phi^{\text{bath}} - \Phi^{\text{gel}}) = -z_f \phi_f \exp \left[\mathcal{G} \left(\frac{1}{\lambda_z} - \frac{1}{J^{\text{gel}}} \right) + \frac{1}{J^{\text{gel}}} (1 - \chi \phi_s^{\text{gel}}) \right], \quad (5.3c)$$

where $\phi_f = \varphi_f / J^{\text{gel}}$ and J^{gel} is given by (2.3). When the cation fraction in the bath is small, $\phi_+^{\text{bath}} \ll 1$, the nonlinear system (5.3) can be reduced to a single equation, as described in Appendix E.

We numerically solve the nonlinear system of algebraic equations defining the outer problem (i.e. the homogeneous equilibria) given by (5.3) using pseudo-arclength continuation. The results are shown as solid curves in Fig. 3 for three different values of $\lambda_z \leq 1$, corresponding to gels in axial compression. The dashed black line represents numerical solutions to the reduced model derived in Appendix E. The figure shows there are two distinct solution branches, one of which describes highly swollen gels ($J^{\text{gel}} > 10$), whereas the other corresponds to weakly swollen gels ($J^{\text{gel}} \sim 1.4$). We refer to the former and latter as the swollen and collapsed branches, respectively. The swollen branch folds back on itself at a critical salt concentration, indicating that a volume phase transition can occur in this system as the salt concentration increases in the bath, which leads to a discontinuous decrease in the gel volume. Increasing the axial compression reduces the degree of swelling for a given salt fraction as well as the critical salt fraction at which the volume phase transition occurs, in agreement with experimental observations [13]. Due to the incompressibility of the gel, imposing an axial compression results in a radial stretch. The elastic energy cost of inserting a molecule into a pre-stretched gel is greater than for a dry (or unstretched) gel. Hence, the balance between the mixing and elastic energies is established at smaller concentrations, resulting in the equilibrium swelling ratio J^{gel} decreasing with the axial stretch λ_z .

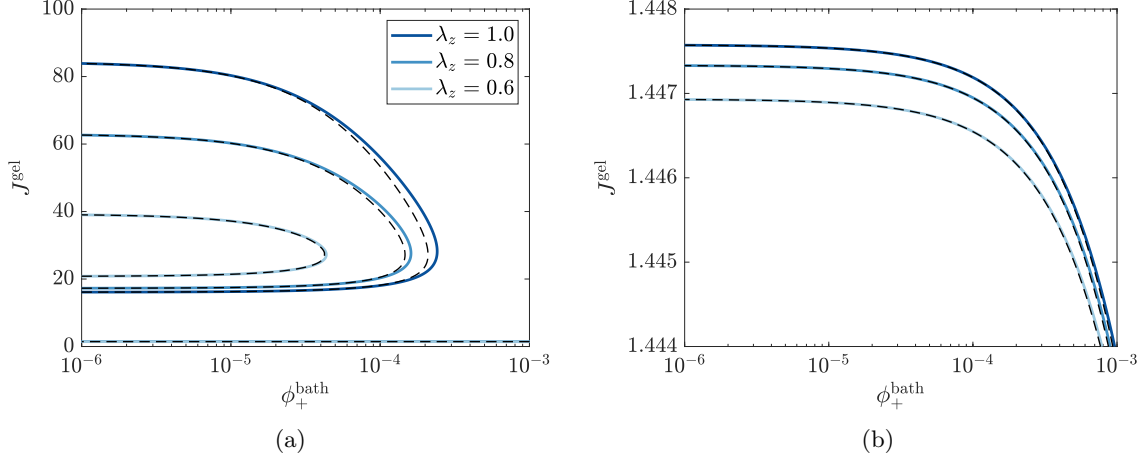


Figure 3: (a) Equilibrium swelling ratio J^{gel} as a function of cation fraction in the bath ϕ_+^{bath} showing swollen and collapsed branches. (b) The swelling ratio along the collapsed branch. Solid lines correspond to solutions of (5.3). Dashed lines represent solutions to the reduced equation (E.4) for a dilute concentration of cations. The parameter values are $\mathcal{G} = 0.0005$, $\chi = 1.2$, $\varphi_f = 0.05$, $z_{\pm} = \pm 1$, $z_f = 1$.

5.2 Formulation of the inner problem

The self-contained inner problem for the gel is formulated by accounting for non-homogeneous deformations in the EDL due to composition gradients. The deformation gradient (5.1) is expanded as $\tilde{\mathbf{F}}^{(0)} = \tilde{\lambda}_r^{(0)} \mathbf{n} \otimes \mathbf{N} + \tilde{\lambda}_{\theta}^{(0)} \mathbf{t}_1 \otimes \mathbf{T}_1 + \lambda_z \mathbf{t}_2 \otimes \mathbf{T}_2$. By matching to (5.2) as $\xi \rightarrow -\infty$ using the conditions in (3.54), we find that $\tilde{\lambda}_{\theta}^{(0)} = (J^{\text{gel}}/\lambda_z)^{1/2}$. By calculating $\tilde{J}^{(0)} = \det \tilde{\mathbf{F}}^{(0)}$ it is possible to eliminate $\tilde{\lambda}_r^{(0)}$ and hence write the deformation gradient tensor as

$$\tilde{\mathbf{F}}_{\parallel}^{(0)} = \tilde{J}^{(0)} \left(\frac{1}{\lambda_z J^{\text{gel}}} \right)^{1/2} \mathbf{n} \otimes \mathbf{N} + \left(\frac{J^{\text{gel}}}{\lambda_z} \right)^{1/2} \mathbf{t}_1 \otimes \mathbf{T}_1 + \lambda_z \mathbf{t}_2 \otimes \mathbf{T}_2. \quad (5.4)$$

The radial elastic stress can be calculated from (3.59a) as

$$\tilde{\mathbf{T}}_{e,rr}^{(0)} = \mathbf{n} \cdot \tilde{\mathbf{T}}_e^{(0)} \cdot \mathbf{n} = \frac{1}{\lambda_z} \frac{\tilde{J}^{(0)}}{J^{\text{gel}}} - \frac{1}{\tilde{J}^{(0)}}, \quad (5.5)$$

which allows the pressure to be determined from (3.61).

The inner problem for the gel can now be constructed using the results from the previous sections. In particular, if $\omega = 0$, then the governing equations for the gel can be condensed into

$$\log \tilde{\phi}_s^{(0)} + \frac{1}{\tilde{J}^{(0)}} + \frac{\chi(1 - \tilde{\phi}_s^{(0)})}{\tilde{J}^{(0)}} + \mathcal{G}\tilde{p}^{(0)} = \log(1 - 2\phi_+^{\text{bath}}), \quad (5.6a)$$

$$\tilde{\phi}_{\pm}^{(0)} = \phi_+^{\text{bath}} \exp \left[\pm (\Phi^{\text{bath}} - \tilde{\Phi}^{(0)}) - \mathcal{G}\tilde{p}^{(0)} - \frac{1}{\tilde{J}^{(0)}} (1 - \chi\tilde{\phi}_s^{(0)}) \right], \quad (5.6b)$$

$$-\frac{\partial^2 \tilde{\Phi}^{(0)}}{\partial \xi^2} = \tilde{\phi}_+^{(0)} - \tilde{\phi}_-^{(0)} + z_f \tilde{\phi}_f^{(0)}, \quad (5.6c)$$

$$\tilde{p}^{(0)} = \frac{1}{\lambda_z} \frac{\tilde{J}^{(0)}}{J^{\text{gel}}} - \frac{1}{\tilde{J}^{(0)}} + \frac{1}{2\mathcal{G}} \left(\frac{\partial \tilde{\Phi}^{(0)}}{\partial \xi} \right)^2, \quad (5.6d)$$

$$\tilde{J}^{(0)} = (1 - \tilde{\phi}_s^{(0)} - \tilde{\phi}_+^{(0)} - \tilde{\phi}_-^{(0)})^{-1}, \quad (5.6e)$$

where $\tilde{\phi}_f^{(0)} = \varphi_f / \tilde{J}^{(0)}$. In the case $\omega \gg \beta$, Eqn (5.6a) is replaced with $\tilde{\phi}_s^{(0)} = \phi_s^{\text{gel}}$, resulting in the system

$$\tilde{\phi}_{\pm}^{(0)} = \phi_+^{\text{bath}} \exp \left[\pm (\Phi^{\text{bath}} - \tilde{\Phi}^{(0)}) - \mathcal{G} \tilde{p}^{(0)} - \frac{1}{\tilde{J}^{(0)}} \left(1 - \chi \phi_s^{\text{gel}} \right) \right], \quad (5.7a)$$

$$-\frac{\partial^2 \tilde{\Phi}^{(0)}}{\partial \xi^2} = \tilde{\phi}_+^{(0)} - \tilde{\phi}_-^{(0)} + z_f \tilde{\phi}_f^{(0)}, \quad (5.7b)$$

$$\mathcal{G} (1 - \phi_s^{\text{gel}}) \tilde{p}^{(0)} = \mathcal{G} \left(\frac{1}{\lambda_z} \frac{\tilde{J}^{(0)}}{J^{\text{gel}}} - \frac{1}{\tilde{J}^{(0)}} \right) + \phi_s^{\text{gel}} \left(\tilde{\Pi}_s^{(0)} - M_s \right) + \frac{1}{2} \left(\frac{\partial \tilde{\Phi}^{(0)}}{\partial \xi} \right)^2, \quad (5.7c)$$

$$\tilde{J}^{(0)} = (1 - \phi_s^{\text{gel}} - \tilde{\phi}_+^{(0)} - \tilde{\phi}_-^{(0)})^{-1}, \quad (5.7d)$$

$$\tilde{\Pi}_s^{(0)} = \log \phi_s^{\text{gel}} + \frac{\chi (1 - \phi_s^{\text{gel}})}{\tilde{J}^{(0)}} - \frac{1}{\tilde{J}^{(0)}}, \quad (5.7e)$$

where $M_s = \mu_s^{\text{bath}} = \log(1 - 2\phi_+^{\text{bath}})$. In both cases, the boundary conditions for the electrical potential are given by (3.64). Moreover, the expression for the hoop stress in the gel, $\tilde{\mathbf{T}}_{\theta\theta}^{(0)} = \mathbf{t}_1 \cdot \tilde{\mathbf{T}}^{(0)} \cdot \mathbf{t}_1$, is the same in both cases as well:

$$\tilde{\mathbf{T}}_{\theta\theta}^{(0)} = \frac{1}{\lambda_z} \left(\frac{J^{\text{gel}}}{\tilde{J}^{(0)}} - \frac{\tilde{J}^{(0)}}{J^{\text{gel}}} \right) - \mathcal{G}^{-1} \left(\frac{\partial \tilde{\Phi}^{(0)}}{\partial \xi} \right)^2. \quad (5.8)$$

The first term represents the elastic contribution to the total hoop stress, which can be compressive or tensile. The second term captures the contribution from the Maxwell stresses, which is always compressive.

5.3 Validation of the asymptotic solution to the inner problem

The systems (5.6) and (5.7) are discretised using finite differences and solved using Newton's method. Once the inner problem in the gel is solved, the electric potential in the bath can be obtained by integrating (3.34) and imposing continuity at the interface. To validate the asymptotic approach, we also solve the full steady problem in axisymmetric cylindrical coordinates, details of which are provided in Appendix F.

We consider the case where the axial stretch and salt content in the bath are set to $\lambda_z = 1$ and $\phi_+^{\text{bath}} = 10^{-5}$, with the remaining parameters being the same as those in Fig. 3. There are three possible solutions to the outer problem. We are only concerned with two of these, which correspond to the collapsed state ($J^{\text{gel}} \simeq 1.447$) and the highly swollen state ($J^{\text{gel}} \simeq 82$). The other solution, which has a swelling ratio $J^{\text{gel}} \simeq 60$, is expected to be unstable [3]. In this subsection, we focus on the inner solution when the outer solution corresponds to the collapsed state. In Sec. 5.4, we explore how the solution to the inner problem is affected by the choice of outer solution.

The inner solution that is computed by matching to the collapsed state is compared with the solution of the full steady problem in Fig. 4. The non-dimensional Debye thickness has been set to $\beta = 10^{-3}$. Although this is higher than the estimate given in Sec. 2.4, it facilitates the numerical solution of the full model. The solutions are plotted in terms of the radial coordinate r , which acts as the outer variable for this geometry. The outer and inner variables are related by $r = a + \beta \xi$. Due to the formulation of the model in terms of Eulerian coordinates, the gel radius a is a free boundary. In the full steady problem, a is calculated as part of the numerical solution; in the asymptotic framework, it is determined from the outer solution as $a = (J^{\text{gel}})^{1/2}$.

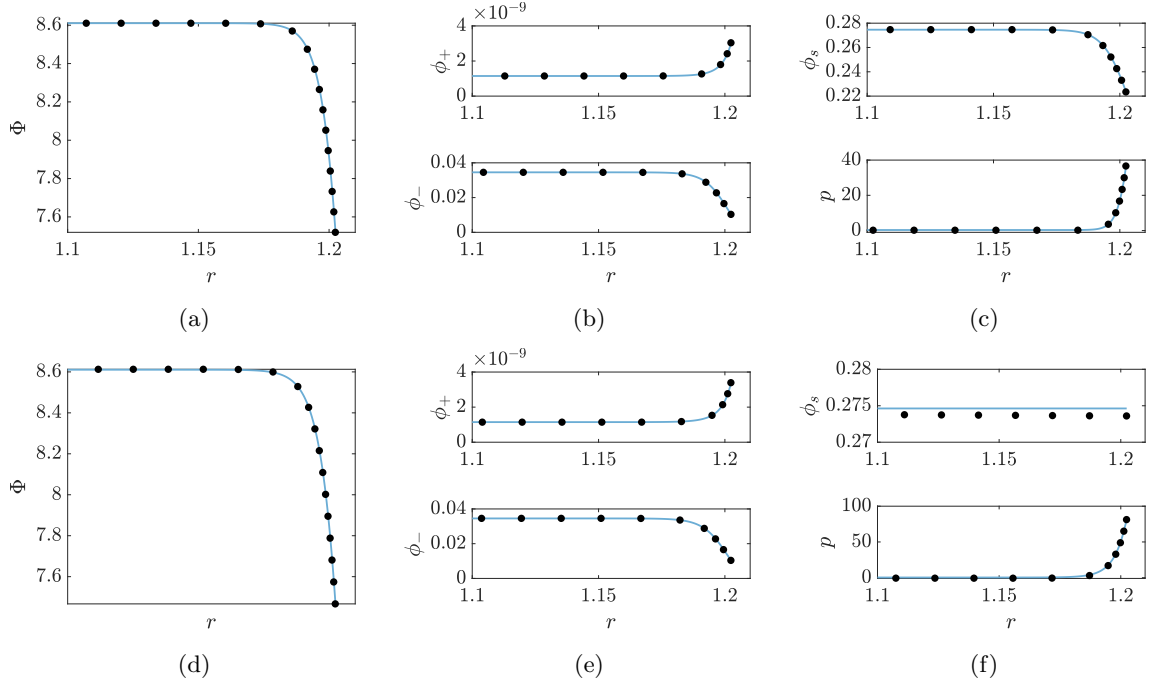


Figure 4: Numerical solutions of the inner problem (lines) and the full steady problem (circles) showing the structure of the EDL. Only the solution to the gel problem is shown. The parameter values are $\chi = 1.2$, $\mathcal{G} = 5 \cdot 10^{-4}$, $\varphi_f = 0.05$, $\phi_+^{\text{bath}} = 10^{-5}$, $\lambda_z = 1$, $\epsilon_r = 1$, $z_{\pm} = \pm 1$, $z_f = 1$, and $\beta = 10^{-3}$. Panels (a)–(c) correspond to the case when $\omega = 0$. Panels (d)–(f) correspond to the case when $\omega = 0.5 \gg \beta$.

In Fig. 4 (a)–(c), we compare the solutions of the full steady problem (circles) and the inner problem (lines) when $\omega = 0$. The electric potential shown in Fig. 4 (a) indicates that the choice of non-dimensionalisation underestimates the width of the EDL, which is roughly 0.025 or 25β . This underestimation is due to the non-dimensionalisation not accounting for the small volume fractions of ions in the EDL; see Fig. 4 (b). Despite this, the solutions to the inner problem and the full problem are in excellent agreement.

The comparison between the inner and full solutions in the case of $\omega \gg \beta$ is shown in Fig. 4 (d)–(f). To ensure a sufficient separation between the Debye length and the width of diffuse interfaces, we have taken $\omega = 0.5 = 500\beta$. Overall, there is good agreement between the solutions, with the main discrepancy occurring in the solvent fraction; see Fig. 4 (f).

5.4 Investigating the structure of the electric double layer

The inner solution is now used to explore the structure of the EDL and how this depends on the outer solution, i.e., the degree of swelling that occurs in the bulk of the gel. We begin by fixing the parameter values to be those in Fig. 3 with $\lambda_z = 1$ and $\phi_+^{\text{bath}} = 10^{-5}$. We then solve the inner problem by matching to the two outer solutions that represent the collapsed and highly swollen states described in Sec. 5.3.

In Fig. 5, we plot the inner solutions when the outer solution corresponds to the collapsed state. The solid and dashed lines correspond to the cases $\omega \gg \beta$ and $\omega = 0$, respectively. For this parameter set, the value of ω does not lead to noticeable changes in the electric potential and ion fractions; see Fig. 5 (a)–(b). However, substantial differences arise in the gel pressure and the solvent fraction; see Fig. 5 (c)–(d). In the case when $\omega = 0$, the gel pressure balances a large Maxwell stress. This large pressure causes a local decrease in the solvent fraction and a minor collapse of the gel (Fig. 4 (c)), which can be rationalised in terms of (4.1a). At equilibrium, the

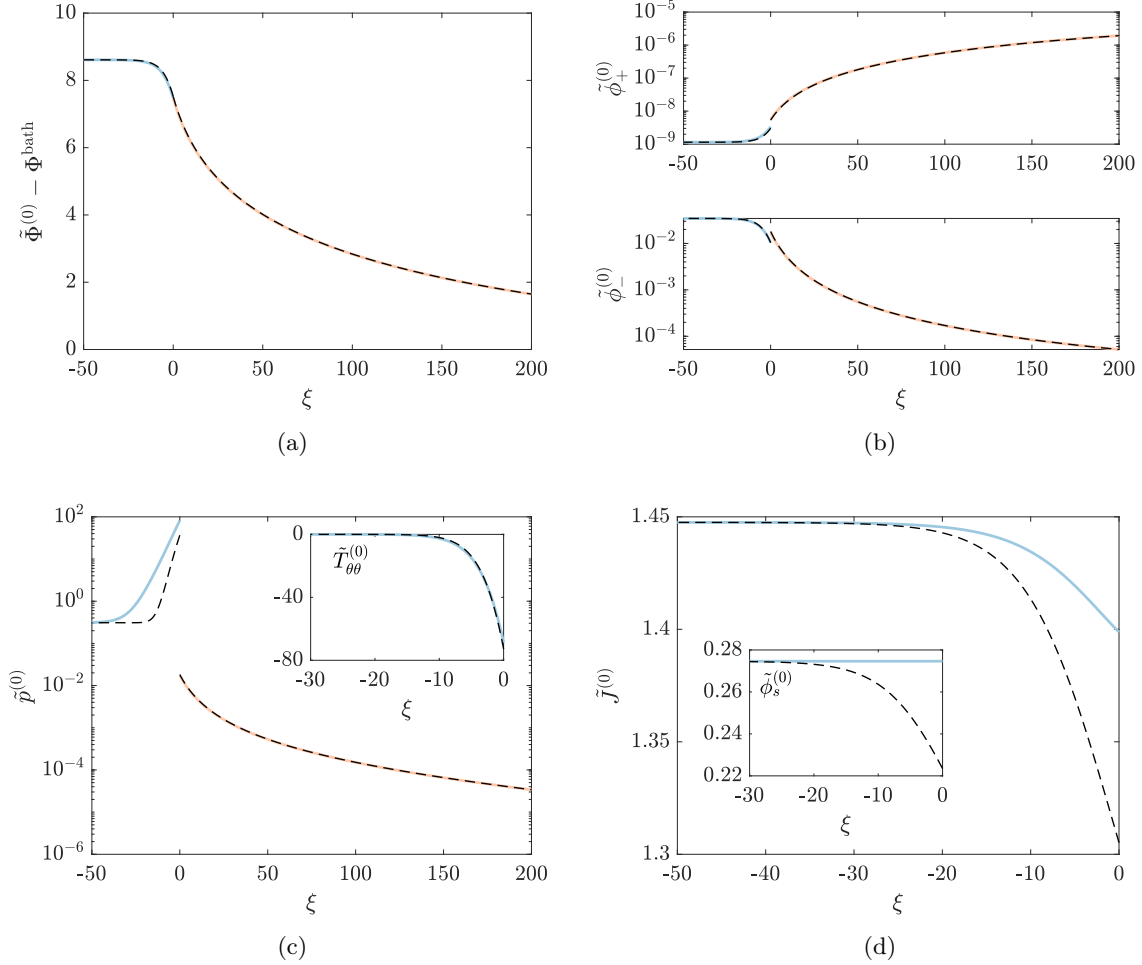


Figure 5: Numerical solution of the inner problem with far-field conditions corresponding to the collapsed state. Solid and dashed lines represent solutions to models with $\omega \gg \beta$ and $\omega = 0$, respectively. Parameters: $\chi = 1.2$, $\mathcal{G} = 0.0005$, $\varphi_f = 0.05$, $\phi_+^{\text{bath}} = 10^{-5}$, $\lambda_z = 1$, $\epsilon_r = 1$, $z_{\pm} = \pm 1$, and $z_f = 1$.

osmotic pressure $\tilde{\Pi}_s$ must balance the mechanical pressure \tilde{p} . To compensate for the increase in mechanical pressure that arises from the Maxwell stresses, the osmotic pressure must decrease, which drives solvent out of the gel and causes it to shrink. When $\omega \gg \beta$, gradients in the solvent fraction are energetically penalised; thus, the solvent fraction remains uniform across the EDL. From a mechanical perspective, this penalisation occurs through the development of a large Korteweg stress, which counters the opposing effects of the Maxwell stress in order to maintain a uniform solvent fraction. The mechanical contribution from the Korteweg stress manifests as an increase in the gel pressure compared to the $\omega = 0$ case, as seen in Fig. 5 (c). Although the solvent fraction is constant across the EDL when $\omega \gg \beta$, the swelling ratio still decreases relative to the bulk value (Fig. 5 (c)) due to the variation in ionic content (Fig. 5 (b)).

The inset of Fig. 5 (c) shows the total hoop stress in the gel, which is the same in both models owing to the strong similarities in the electric potential. Due to the large Maxwell stresses, the gel experiences a substantial compressive hoop stress, which leads to the intriguing possibility of localised mechanical instabilities in the EDL.

In Fig. 6, we show the numerical solution of the inner problem with $\omega \gg \beta$ when the outer solution corresponds to the highly swollen state. The qualitative features of the solution are similar to those shown in Fig. 5, where the outer solution corresponds to the collapsed state.

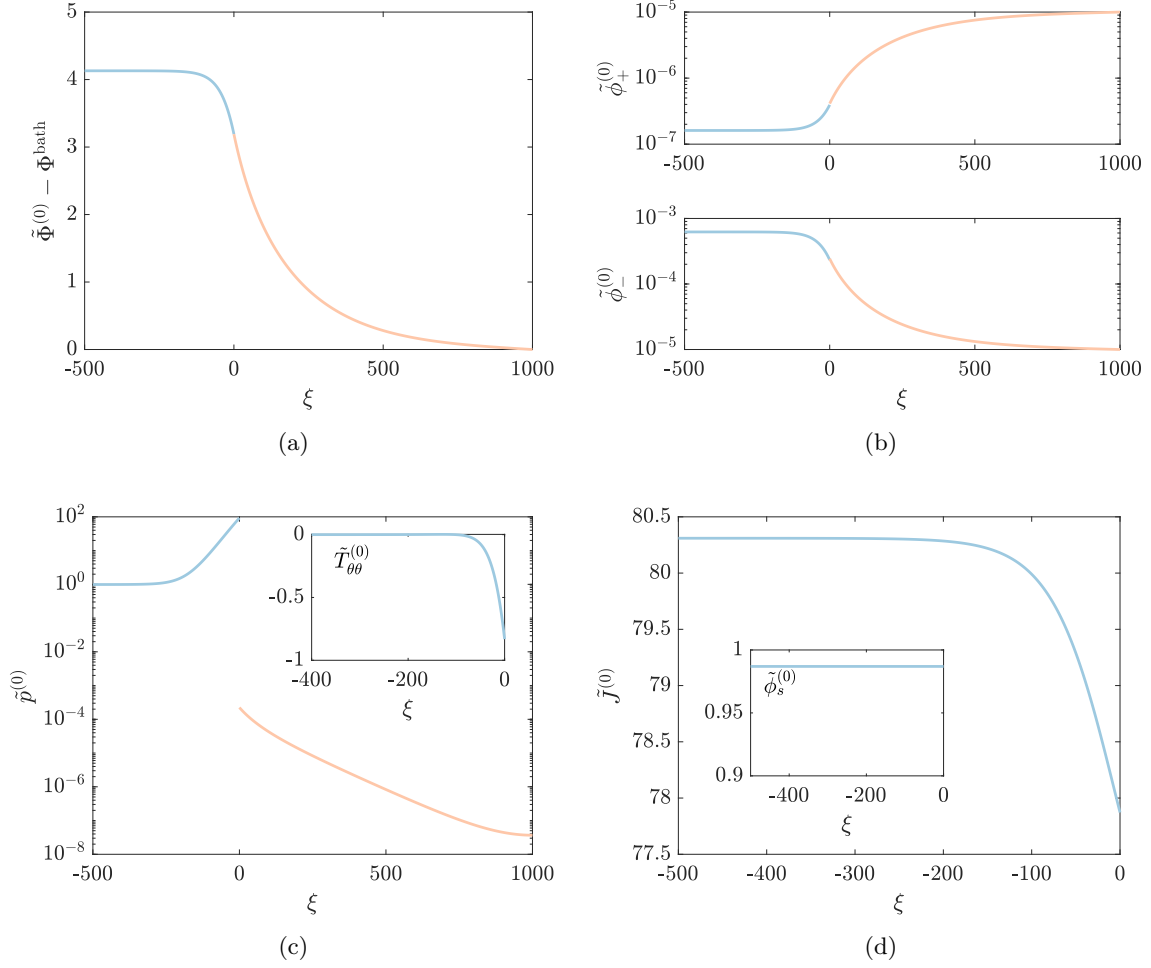


Figure 6: Numerical solution of the inner problem with far-field conditions corresponding to the swollen state when $\omega \gg \beta$. Parameter values are the same as in Fig. 5: $\chi = 1.2$, $\mathcal{G} = 0.0005$, $\varphi_f = 0.05$, $\phi_+^{\text{bath}} = 10^{-5}$, $\lambda_z = 1$, $\epsilon_r = 1$, $z_{\pm} = \pm 1$, and $z_f = 1$.

However, an important difference is that the concentration of anions has decreased by more than a factor of ten due to the reduction in the volume fraction of fixed charges when the gel is highly swollen. Consequently, the EDL in the gel has increased in thickness by a roughly factor of ten to approximately 250β (or 25 nm). The gradient in the electric potential in the gel is therefore ten times weaker, resulting in a 100-fold reduction in the Maxwell stresses and the total hoop stress. Despite these decreases, the pressure in the gel remains large because of the Korteweg stresses. Due to convergence issues, it was not possible to compute the corresponding inner solution when $\omega = 0$.

To understand the origin of these numerical difficulties, we consider an intermediate asymptotic limit where $\omega = \Omega\beta$, with $\Omega = O(1)$ as $\beta \rightarrow 0$. Full details of this limit are beyond the scope of this work; however, for the purpose of this discussion it suffices to say that the inner problem in the gel amounts to changing (3.43) or (4.1a) to

$$\tilde{\Pi}_s^{(0)} + \mathcal{G}\tilde{p}^{(0)} + \Omega^2 \frac{\partial^2 \tilde{\phi}_s^{(0)}}{\partial \xi^2} = \mu_s^{\text{bath}}, \quad (5.9a)$$

where we have used the equality of the equilibrium chemical potentials $\mu_s^{\text{gel}} = \mu_s^{\text{bath}}$. The

pressure (3.61) can be evaluated using a Korteweg stress given by

$$\mathbf{n} \cdot \tilde{\mathbf{T}}_K^{(0)} \cdot \mathbf{n} = \mathcal{G}^{-1} \Omega^2 \left[\tilde{\phi}_s^{(0)} \frac{\partial^2 \tilde{\phi}_s^{(0)}}{\partial \xi^2} - \frac{1}{2} \left(\frac{\partial \tilde{\phi}_s^{(0)}}{\partial \xi} \right)^2 \right]. \quad (5.9b)$$

The intermediate asymptotic model was solved using a second parameter set that reduces the degree of swelling that occurs in the gel and forces the the outer problem to have only a single branch of solutions. Thus, the gel monotonically and continuously decreases in volume as the salt fraction in the bath ϕ_+^{bath} increases. The inner problem was solving using the intermediate model at three specific values of ϕ_+^{bath} using a value of $\Omega = 0.1$. The swelling ratio $\tilde{J}^{(0)}$ and total charge $\tilde{Q}^{(0)} = \tilde{\phi}_+^{(0)} - \tilde{\phi}_-^{(0)} + z_f \tilde{\phi}_f^{(0)}$ are computed and plotted as functions of space in Fig. 7. In this case, decreasing the salt fraction in the bath from $\phi_+^{\text{bath}} = 10^{-3}$ triggers the onset of phase separation, which gives rise to an array of electrically charged structures that spans the entire domain of the inner problem. Charge neutrality is not recovered in the far field, even if the domain used to numerically solve the inner problem is increased, meaning that the inner solution cannot be matched with the homogeneous outer solutions computed from (5.3). We therefore posit that homogeneous outer solutions do not always exist in the limit $\beta \rightarrow 0$ with $\omega = O(\beta)$ or $\omega = 0$. The lack of a homogeneous outer solution could explain the difficulties in numerically solving the inner problem using the same parameters as in Fig. 6 when $\omega = 0$.

To explore the hypothesis that the bulk of the gel may not be homogeneous and electrically neutral at equilibrium, we solved the full steady problem with $\beta = 10^{-2}$ and $\omega = 10^{-3}$. The salt fraction in the bath was set to $\phi_+^{\text{bath}} = 6.6 \cdot 10^{-4}$, corresponding to the parameters in Fig. 7 (b) and (e). The swelling ratio J and the total charge Q , which are shown in Fig. 8, reveal that phase separation occurs throughout the entire gel and gives rise to a periodic arrangement of electrically charged domains. Using numerical integration, we find that the total amount of electric charge contained within a pair of adjacent domains is on the order of 10^{-7} . Thus, the gel effectively separates into three distinct regions consisting of an electrically negative, highly swollen core ($0 < r < 0.73$); a moderately swollen interior that is electrically neutral on average ($0.073 < r < 2.0$); and a positively charged, collapsed shell ($2.0 < r < 2.1$). Overall, the gel carries a net positive charge which exactly balances the net negative charge in the bath to ensure that charge neutrality holds on a global scale. The pointwise breakdown of charge neutrality across the gel indicates that it is not always appropriate to decompose the problem into inner and outer regions that are characterised by the local charge density of the gel.

6 Discussion and conclusion

Asymptotic and numerical methods are used to study the EDL that forms at the interface between a salt bath and a polyelectrolyte gel. The gel is described using a phase-field model, which introduces an additional length scale, the Kuhn length, into the problem. The Kuhn length measures the thickness of diffuse internal interfaces that can form due to phase separation within the gel. The ratio of the non-dimensional Kuhn and Debye lengths, ω and β , has a profound influence on the structure of equilibrium solutions that has not been reported before.

When $\omega \gg \beta$, there is a high energy cost associated with gradients in the solvent concentration. Therefore, the leading-order solvent volume fraction is uniform across the EDL. Importantly, the complex interplay between mechanics, electrostatics, and thermodynamics, which can result in phase separation, is suppressed. This interplay is captured in the contributions to the solvent chemical potential from the osmotic and mechanical pressures, which do not enter at leading order. When applying the asymptotic framework to a cylindrical gel, it

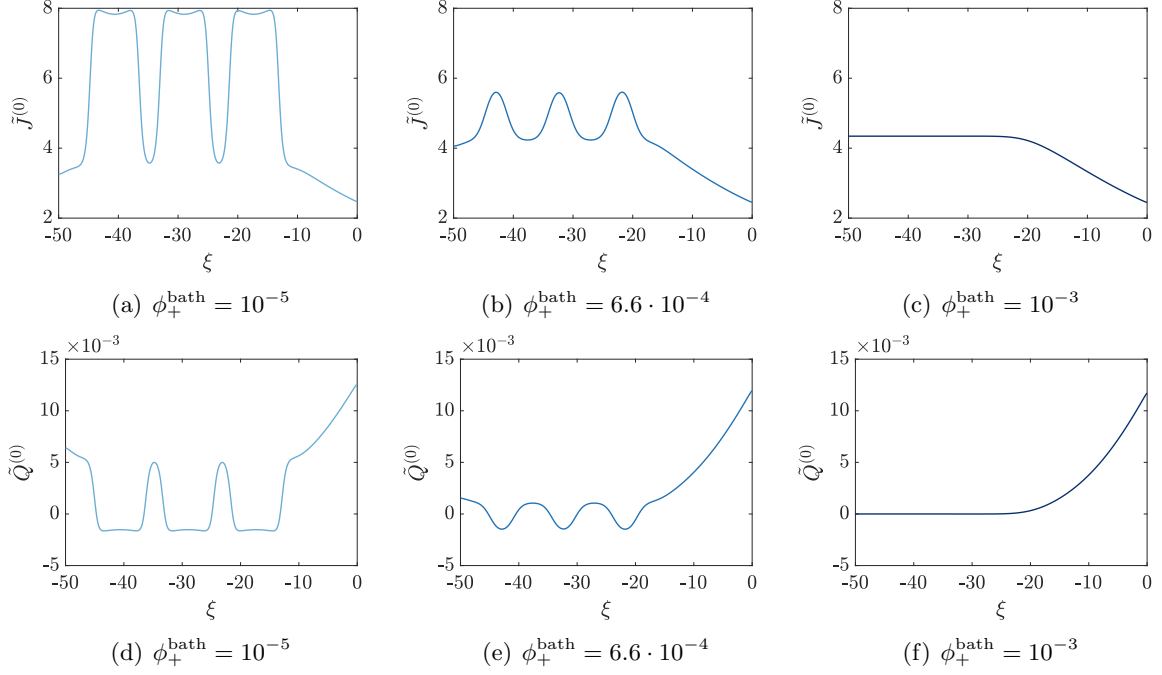


Figure 7: Phase separation in the inner region. (a)–(c) The swelling ratio and (d)–(f) the total electric charge computed using the intermediate asymptotic model when the Debye length is comparable to the Kuhn length. We have taken $\omega = \Omega\beta$ with $\Omega = 10^{-1}$. The remaining parameters are $\chi = 0.7$, $\mathcal{G} = 4 \cdot 10^{-3}$, $\varphi_f = 0.04$, $z_{\pm} = \pm 1$, $z_f = 1$, $\epsilon_r = 1$, and $\lambda_z = 1$.

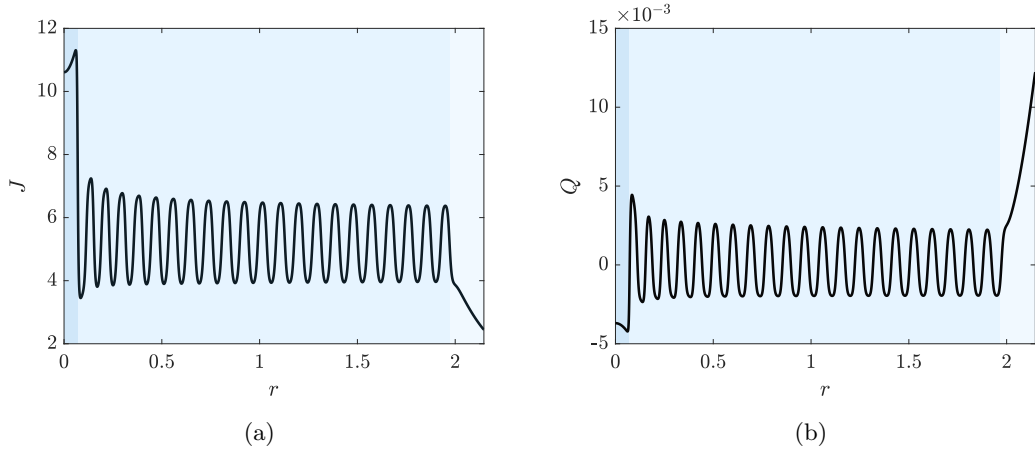


Figure 8: Phase separation drives the breakdown of charge neutrality in the gel when the Debye length is comparable to the Kuhn length. (a) The swelling ratio and (b) the total electric charge computed from the full steady problem in cylindrical coordinates. The parameter values are $\beta = 10^{-2}$, $\omega = 10^{-3}$, $\phi_+^{\text{bath}} = 6.6 \cdot 10^{-4}$, $\chi = 0.7$, $\mathcal{G} = 4 \cdot 10^{-3}$, $\varphi_f = 0.04$, $z_{\pm} = \pm 1$, $z_f = 1$, $\epsilon_r = 1$, and $\lambda_z = 1$.

is possible to match the inner solutions to electrically neutral, homogeneous outer solutions in all of the considered cases. In contrast, when $\omega = 0$, the leading-order solvent fraction in the EDL is set by the between the osmotic and mechanical pressures. In this case, it is not always possible to compute a numerical solution to the inner problem.

Our preliminary investigation of the intermediate asymptotic limit where $\beta \rightarrow 0$ with $\omega = O(\beta)$ reveals that phase separation can result in highly heterogeneous gels consisting of repeating pairs of positively and negatively charged domains. The breakdown of charge neutrality means that the inner region effectively spans the entire gel. The difficulties in numerically computing inner solutions with $\omega = 0$ are therefore attributed to the gel undergoing phase separation and the loss of homogeneous outer solutions.

In Celora *et al.* [4], we used continuation methods to track numerical solutions of the full steady problem as the salt fraction in the bath is varied in the regime when ω and β are comparable. We found that the breakdown of charge neutrality in the gel occurs via a cascade of saddle-node bifurcations associated with spatially localised modes of phase separation. A more in-depth analysis of the asymptotic limit $\beta \rightarrow 0$ with $\omega = O(\beta)$ and the bifurcation structure will be an interesting and insightful area of future work.

Physically, the breakdown of electroneutrality due to phase separation when the Kuhn and Debye lengths can be rationalised as follows. Phase separation leads to the formation of diffuse interfaces that separate domains with distinct compositions and electric potentials. The gradient in the electric potential across the diffuse interface generates an electric field. When the Kuhn and Debye lengths are commensurate, the electric field near the diffuse interface will be of sufficient magnitude to trigger the formation of an internal EDL. If the Kuhn length greatly exceeds the Debye length, then the electric field is too weak to generate an EDL and hence the gel remains electrically neutral.

Typical models of polyelectrolyte gels do not account for phase separation and thus implicitly set $\omega = 0$. Homogeneous and hence electrically neutral solutions that neglect the EDL are often sought and compared against experimental data. However, our results show that these homogeneous ‘solutions’ may be asymptotically inconsistent because there is no inner solution in the EDL that can be matched to them. In fact, when $\omega = 0$, the bulk behaviour of the gel can be strongly coupled to the behaviour in the EDL and thus the latter must be considered when constructing model solutions. The extensive use of homogeneous, electroneutral solutions to characterise the response of highly swollen polyelectrolyte gels is more consistent with the assumption that $\omega \gg \beta$, as this limit enables the successful matching of inner and outer solutions and prohibits the breakdown of electroneutrality in the bulk of the gel.

A key outcome of this work is the systematic derivation of an electroneutral model for a polyelectrolyte gel with consistent jump conditions across the gel-bath interface that can capture phase separation. This model was derived in the limit $\beta \rightarrow 0$ with $\beta \ll \omega$. In Celora *et al.* [3], we use our electroneutral model to study the rich variety of dynamics that can occur when a polyelectrolyte gel in contact with a salt bath undergoes phase separation. Given importance of electroneutral models in the applied literature, the results presented in this paper will increase our understanding of how asymptotic methods can be used to derive consistent jump conditions across dynamic EDLs that form at the free interfaces of complex materials, including those which undergo large elastic deformations.

A Summary of the governing equations in dimensional form

A.1 Bulk equations for the gel

Conservation of solvent and ions is given by

$$\frac{\partial c_m}{\partial t} + \nabla \cdot (c_m \mathbf{v}_m) = 0 \quad (\text{A.1})$$

for $m \in \mathbb{M}$, where c_m is the (current) concentration (number of molecules per unit current volume). The velocity \mathbf{v}_m is related to the network velocity \mathbf{v}_n and the diffusive flux \mathbf{j}_m according to

$$c_m(\mathbf{v}_m - \mathbf{v}_n) = \mathbf{j}_m. \quad (\text{A.2})$$

Due to incompressibility, the determinant of the deformation tensor is

$$J = 1 + \sum_{m \in \mathbb{M}} \nu C_m = \left(1 - \sum_{m \in \mathbb{M}} \nu c_m \right)^{-1}, \quad (\text{A.3})$$

where $C_m = Jc_m$ is the nominal concentration of each mobile species and ν is the molecular volume, i.e. the volume of an individual molecule. For simplicity, we assume that all of the molecules are roughly the same size. The diffusive fluxes of the solvent and ions are given by

$$\mathbf{j}_s = -\frac{D_s(J)}{k_B T} \sum_{m \in \mathbb{M}} c_m \nabla \mu_m, \quad (\text{A.4a})$$

$$\mathbf{j}_\pm = -\frac{D_\pm c_\pm}{k_B T} \nabla \mu_\pm + \frac{c_\pm}{c_s} \mathbf{j}_s, \quad (\text{A.4b})$$

where T is temperature, k_B is Boltzmann's constant, D_s is the diffusivity of solvent in a polymer network, and D_\pm are the diffusivity of ions in a pure solvent bath. A common functional form of the solvent diffusivity is $D_s = D_s^0 J^a$ with $a = 1.5$; see Bertrand *et al.* [2]. The chemical potential of solvent can be written as

$$\mu_s = \mu_s^0 + \nu(p + \Pi_s) - \gamma \nabla^2 c \quad (\text{A.5})$$

where p is the mechanical pressure, Π_s is the osmotic pressure of the solvent,

$$\Pi_s = \frac{k_B T}{\nu} \left[\log(\nu c_s) + \frac{\chi(1 - \nu c_s)}{J} + \frac{1}{J} \right], \quad (\text{A.6})$$

and χ is the Flory interaction parameter. The chemical potential of ions is given by

$$\mu_\pm = \mu_\pm^0 + \nu(\Pi_\pm + p) \pm e\Phi, \quad (\text{A.7})$$

where Φ is the electric potential, e is the elementary charge, and Π_\pm is the osmotic pressure

$$\Pi_\pm = \frac{k_B T}{\nu} \left[\log(\nu c_\pm) + \frac{1}{J}(1 - \chi \nu c_s) \right]. \quad (\text{A.8})$$

The quantities μ_m^0 are reference values of the chemical potential. The electric potential satisfies

$$-\epsilon^{\text{gel}} \nabla^2 \Phi = e(c_+ - c_- + z_f c_f) \quad (\text{A.9})$$

where ϵ^{gel} is the electrical permittivity of the gel and c_f is the current concentration of fixed charges. Mechanical equilibrium leads to

$$\nabla \cdot \mathbf{T} = 0, \quad (\text{A.10})$$

where the Cauchy stress tensor \mathbf{T} can be decomposed into four contributions

$$\mathbf{T} = \mathbf{T}_e + \mathbf{T}_K + \mathbf{T}_M - p\mathbf{I}, \quad (\text{A.11})$$

associated with the elastic stress \mathbf{T}_e , the Korteweg stress \mathbf{T}_K , the Maxwell stress \mathbf{T}_M , and the isotropic fluid pressure. These three stress tensors are given by

$$\mathbf{T}_e = GJ^{-1}(\mathbf{B} - \mathbf{I}), \quad (\text{A.12a})$$

$$\mathbf{T}_K = \gamma \left[\left(\frac{1}{2} |\nabla c_s|^2 + c_s \nabla^2 c_s \right) \mathbf{I} - \nabla c_s \otimes \nabla c_s \right], \quad (\text{A.12b})$$

$$\mathbf{T}_M = \epsilon^{\text{gel}} \left(\nabla \Phi \otimes \nabla \Phi - \frac{1}{2} |\nabla \Phi|^2 \mathbf{I} \right), \quad (\text{A.12c})$$

where G and γ play the role of a shear modulus and surface energy, respectively. The left Cauchy–Green tensor is defined as $\mathbf{B} = \mathbf{F}\mathbf{F}^T$. In Eulerian coordinates, the deformation gradient tensor satisfies $\mathbf{F}^{-1} = \nabla \mathbf{X}$. The velocity of the network can be determined from

$$\mathbf{v}_n = -\mathbf{F} \frac{\partial \mathbf{X}}{\partial t}. \quad (\text{A.13})$$

A.2 Governing equations for the bath

Conservation of solvent and ions is given by

$$\frac{\partial c_m}{\partial t} + \nabla \cdot (c_m \mathbf{v}_m) = 0, \quad (\text{A.14})$$

for $m \in \mathbb{M}$. The mixture velocity is defined as

$$\mathbf{v} = \sum_m \nu c_m \mathbf{v}_m. \quad (\text{A.15})$$

Note that we also have

$$\sum_m \nu c_m = 1, \quad \nabla \cdot \mathbf{v} = 0. \quad (\text{A.16})$$

The velocity of each species can be linked to the diffusive flux via

$$c_m (\mathbf{v}_m - \mathbf{v}) = \mathbf{q}_m, \quad (\text{A.17})$$

which implies that

$$\sum_{m \in \mathbb{M}} \mathbf{q}_m = 0. \quad (\text{A.18})$$

The diffusive fluxes are defined by

$$\mathbf{j}_{\pm} = -\frac{D_{\pm} c_{\pm}}{k_B T} \left(\nabla \mu_{\pm} - \nu \sum_{m \in \mathbb{M}} c_m \nabla \mu_m \right) + \frac{c_{\pm}}{c_s} \mathbf{j}_s, \quad (\text{A.19a})$$

$$\mathbf{j}_s = -\mathbf{j}_+ - \mathbf{j}_-. \quad (\text{A.19b})$$

The chemical potentials are given by

$$\mu_s = \mu_s^0 + \nu(\Pi_s + p), \quad (\text{A.20a})$$

$$\mu_{\pm} = \mu_{\pm}^0 + \nu(\Pi_{\pm} + p) \pm e\Phi, \quad (\text{A.20b})$$

where

$$\Pi_m = \frac{k_B T}{\nu} \log(\nu c_m). \quad (\text{A.21})$$

The electric potential satisfies

$$-\epsilon^{\text{bath}} \nabla^2 \Phi = e(c_+ - c_-). \quad (\text{A.22})$$

The stress balance in the bath is given by

$$\nabla \cdot \mathbf{T} = 0, \quad (\text{A.23})$$

where $\mathbf{T} = \mathbf{T}_v + \mathbf{T}_M - p\mathbf{I}$ where

$$\mathbf{T}_v = \eta(\nabla \mathbf{v} + \nabla \mathbf{v}^T), \quad (\text{A.24a})$$

$$\mathbf{T}_M = \epsilon^{\text{bath}} \left(\nabla \Phi \otimes \nabla \Phi - \frac{1}{2} |\nabla \Phi|^2 \mathbf{I} \right). \quad (\text{A.24b})$$

A.3 Boundary conditions at the gel-bath interface

The boundary conditions are discussed in detail in the text. Conservation of solvent and ions across the gel-bath interface are given by

$$[c_m(\mathbf{v}_m \cdot \mathbf{n} - V_n)]_{\mathbf{x}=r^-}^{\mathbf{x}=r^+} = 0, \quad (\text{A.25})$$

where V_n is the normal velocity of the interface. The kinematic boundary condition for the velocity of the polymer network is

$$[\mathbf{v}_n \cdot \mathbf{n} - V_n]_{\mathbf{x}=r^-} = 0. \quad (\text{A.26})$$

Continuity of chemical potential implies that

$$[\mu_m]_{\mathbf{x}=r^-}^{\mathbf{x}=r^+} = 0. \quad (\text{A.27})$$

The variational condition for the solvent concentration is

$$[\nabla c_s \cdot \mathbf{n}]_{\mathbf{x}=r^-} = 0. \quad (\text{A.28})$$

Conservation of normal and tangential momentum gives

$$[\mathbf{T} \cdot \mathbf{n}]_{\mathbf{x}=r^+}^{\mathbf{x}=r^-} = 0. \quad (\text{A.29})$$

The slip condition reads as

$$[\mathbf{v} \cdot \mathbf{t}_i]_{\mathbf{x}=r^-}^{\mathbf{x}=r^+} = 0. \quad (\text{A.30})$$

We impose continuity of electrical potential and electric displacement

$$[\Phi]_{\mathbf{x}=r^-}^{\mathbf{x}=r^+} = 0, \quad (\text{A.31a})$$

$$[-\epsilon \nabla \Phi \cdot \mathbf{n}]_{\mathbf{x}=r^-}^{\mathbf{x}=r^+} = 0. \quad (\text{A.31b})$$

and therefore do not account for surface charges on the gel.

B Conventions and identities

A vector \mathbf{v} is written in component form as $\mathbf{v} = v_i \mathbf{e}_i$. Similarly, a tensor \mathbf{T} is written in component form as $\mathbf{T} = T_{ij} \mathbf{e}_i \otimes \mathbf{e}_j$. The gradient of the vector \mathbf{v} is defined in Cartesian coordinates as

$$\nabla \mathbf{v} = \frac{\partial}{\partial x_j} (v_i \mathbf{e}_i) \otimes \mathbf{e}_j. \quad (\text{B.1})$$

Similarly, the tensor divergence is defined as

$$\nabla \cdot \mathbf{T} = \frac{\partial}{\partial x_i} (T_{jk} \mathbf{e}_j \otimes \mathbf{e}_k) \mathbf{e}_i, \quad (\text{B.2})$$

which can be evaluated using the property of the dyadic product $(\mathbf{a} \otimes \mathbf{b})\mathbf{c} = (\mathbf{b} \cdot \mathbf{c})\mathbf{a}$. Given two vectors $\mathbf{a} = a_i \mathbf{e}_i$ and $\mathbf{b} = b_j \mathbf{e}_j$ and a tensor $\mathbf{T} = T_{kl} \mathbf{e}_k \otimes \mathbf{e}_l$, we write

$$\mathbf{a} \cdot \mathbf{T} \cdot \mathbf{b} = (a_i T_{kl} b_j) (\mathbf{e}_l \cdot \mathbf{e}_j) (\mathbf{e}_i \cdot \mathbf{e}_k), \quad (\text{B.3})$$

which collapses to $a_i T_{ij} b_j$ if the basis vectors are orthonormal.

C Transformation of the derivatives in the inner region

We derive the asymptotic expressions in (3.12) for the time derivative, gradient, and Laplacian in the inner region. We will use the convention of summing over repeated indices. Greek indices range from 1 to 2.

In the inner problem we write

$$\mathbf{x} = \mathbf{r}(s_1, s_2, t) + \beta \xi \mathbf{n}(s_1, s_2, t), \quad (\text{C.1a})$$

$$t = t', \quad (\text{C.1b})$$

where \mathbf{r} denotes the location of the gel-bath interface and \mathbf{n} is the unit normal vector pointing from the gel into the bath. The tangent and normal vectors are defined as

$$\mathbf{t}_\alpha = \frac{\partial \mathbf{r}}{\partial s_\alpha}, \quad \mathbf{n} = \frac{\mathbf{t}_1 \times \mathbf{t}_2}{\|\mathbf{t}_1 \times \mathbf{t}_2\|}. \quad (\text{C.2})$$

The normal velocity of the interface is defined as $V_n = \mathbf{n} \cdot \partial_{t'} \mathbf{r}$.

Before proceeding with the transformation, it is helpful to summarise some key definitions and results from differential geometry. The components of the metric tensor are defined as $g_{\alpha\nu} = \mathbf{t}_\alpha \cdot \mathbf{t}_\nu$. We let $g^{\alpha\nu}$ denote the components of the inverse of the metric tensor. The curvature tensor has components

$$K_{\alpha\nu} = -\mathbf{n} \cdot \frac{\partial \mathbf{t}_\alpha}{\partial s_\nu} = \frac{\partial \mathbf{n}}{\partial s_\nu} \cdot \mathbf{t}_\alpha. \quad (\text{C.3})$$

The metric tensor, its inverse, and the curvature tensor are all symmetric. The shape operator is defined as $S_\nu^\gamma = g^{\gamma\alpha} K_{\alpha\nu}$. The eigenvalues of the shape operator, κ_1 and κ_2 , define the principal curvatures of the surface. Similarly, the trace of the shape operator is related to the mean curvature of the surface, $\kappa = (\kappa_1 + \kappa_2)/2$, through the relation $S_\alpha^\alpha = 2\kappa$. By ensuring that the normal vector \mathbf{n} computed from (C.2) points into the bath, the principal curvatures of a spherical gel will be positive.

A straightforward application of the chain rule shows that

$$\frac{\partial}{\partial s_\alpha} = \left(\mathbf{t}_\alpha + \beta \xi \frac{\partial \mathbf{n}}{\partial s_\alpha} \right) \cdot \nabla, \quad (\text{C.4})$$

$$\frac{\partial}{\partial \xi} = \beta \mathbf{n} \cdot \nabla, \quad (\text{C.5})$$

$$\frac{\partial}{\partial t'} = \frac{\partial}{\partial t} + \left(\frac{\partial \mathbf{r}}{\partial t'} + \beta \xi \frac{\partial \mathbf{n}}{\partial t'} \right) \cdot \nabla. \quad (\text{C.6})$$

We now exploit the fact that $\beta \ll 1$ and write the differential operators ∇ and ∂_t as asymptotic series of the form $\nabla = \beta^{-1} \nabla^{(-1)} + \nabla^{(0)} + \beta \nabla^{(1)} + O(\beta^2)$ and $\partial_t = \beta^{-1} \partial_t^{(-1)} + \partial_t^{(0)} + O(\beta)$.

The $O(\beta^{-1})$ problem for the del operator is

$$0 = \mathbf{t}_\alpha \cdot \nabla^{(-1)}, \quad (\text{C.7a})$$

$$\frac{\partial}{\partial \xi} = \mathbf{n} \cdot \nabla^{(-1)}, \quad (\text{C.7b})$$

which has the solution

$$\nabla^{(-1)} = \mathbf{n} \frac{\partial}{\partial \xi}. \quad (\text{C.8})$$

The corresponding problem for the time derivative is trivial to solve and has solution

$$\partial_t^{(-1)} = -V_n \frac{\partial}{\partial \xi}. \quad (\text{C.9})$$

The $O(1)$ problem for the del operator is given by

$$\frac{\partial}{\partial s_\alpha} = \mathbf{t}_\alpha \cdot \nabla^{(0)} + \xi \mathbf{n} \cdot \frac{\partial \mathbf{n}}{\partial s_\alpha} \frac{\partial}{\partial \xi}, \quad (\text{C.10a})$$

$$0 = \mathbf{n} \cdot \nabla^{(0)}. \quad (\text{C.10b})$$

Since \mathbf{n} is a unit vector, we have that $\mathbf{n} \cdot \partial_{s_\alpha} \mathbf{n} = (1/2) \partial_{s_\alpha} (\mathbf{n} \cdot \mathbf{n}) = 0$, implying the final term in (C.10a) vanishes. Equation (C.10b) implies that $\nabla^{(0)}$ lies in the tangent plane and thus has the form $\nabla^{(0)} = a_\alpha \mathbf{t}_\alpha$. Inserting this solution in (C.10a) and solving gives

$$\nabla^{(0)} = g^{\alpha\nu} \mathbf{t}_\alpha \frac{\partial}{\partial s_\nu} \equiv \nabla_s, \quad (\text{C.11})$$

where ∇_s is the surface gradient. The $O(1)$ contribution to the time derivative can be calculated as

$$\partial_t^{(0)} = \frac{\partial}{\partial t'} - \frac{\partial \mathbf{r}}{\partial t'} \cdot \nabla_s. \quad (\text{C.12})$$

The $O(\beta)$ problem for the del operator, after minor simplification, is given by

$$\mathbf{t}_\alpha \cdot \nabla^{(1)} = -\xi \frac{\partial \mathbf{n}}{\partial s_\alpha} \cdot \nabla^{(0)}, \quad (\text{C.13a})$$

$$\mathbf{n} \cdot \nabla^{(1)} = 0. \quad (\text{C.13b})$$

By following the same strategy as the $O(1)$ problem, substituting the solution in (C.11), and using (C.3) and the definition of the shape operator, we find that

$$\nabla^{(1)} = -\xi S_\gamma^\alpha g^{\gamma\nu} \mathbf{t}_\alpha \frac{\partial}{\partial s_\nu}. \quad (\text{C.14})$$

Using these asymptotic expansions, we can construct the Laplacian $\nabla^2 = \nabla \cdot \nabla$. In doing so, we will use the fact that the tangent and normal vectors \mathbf{t}_α and \mathbf{n} are independent of the coordinate ξ . As a result, $\nabla^{(-1)} \cdot \nabla^{(-1)} = \partial_{\xi\xi}$, $\nabla^{(-1)} \cdot \nabla^{(0)} = 0$, and $\nabla^{(-1)} \cdot \nabla^{(1)} = 0$. Moreover,

$$\nabla^{(0)} \cdot \nabla^{(-1)} = g^{\alpha\nu} \mathbf{t}_\alpha \cdot \frac{\partial \mathbf{n}}{\partial s_\nu} \frac{\partial}{\partial \xi} = S_\alpha^\alpha \frac{\partial}{\partial \xi} = 2\kappa \frac{\partial}{\partial \xi}, \quad (\text{C.15a})$$

$$\nabla^{(0)} \cdot \nabla^{(0)} = g^{\alpha\nu} \mathbf{t}_\alpha \cdot \frac{\partial}{\partial s_\nu} \left(g^{\gamma\delta} \mathbf{t}_\gamma \frac{\partial}{\partial s_\delta} \right) = g^{\alpha\nu} g^{\gamma\delta} \mathbf{t}_\alpha \cdot \frac{\partial \mathbf{t}_\gamma}{\partial s_\nu} \frac{\partial}{\partial s_\delta} + \frac{\partial}{\partial s_\gamma} \left(g^{\gamma\delta} \frac{\partial}{\partial s_\delta} \right). \quad (\text{C.15b})$$

In order to simplify (C.15b), we express the derivatives of the tangent vectors as

$$\frac{\partial \mathbf{t}_\gamma}{\partial s_\nu} = \Gamma_{\gamma\nu}^\epsilon \mathbf{t}_\epsilon - K_{\gamma\nu} \mathbf{n}, \quad (\text{C.16})$$

where $\Gamma_{\gamma\nu}^\epsilon$ is the Christoffel symbol. In addition, we invoke the identity

$$\Gamma_{\gamma\alpha}^\alpha = \frac{1}{\sqrt{g}} \frac{\partial}{\partial s_\gamma} (\sqrt{g}), \quad (\text{C.17})$$

where $g = g_{11}g_{22} - g_{12}^2$ is the determinant of the metric tensor. Thus, we find that $\nabla^{(0)} \cdot \nabla^{(0)} = \nabla_s^2$, where

$$\nabla_s^2 = \frac{1}{\sqrt{g}} \frac{\partial}{\partial s_\gamma} \left(\sqrt{g} g^{\gamma\delta} \frac{\partial}{\partial s_\delta} \right) \quad (\text{C.18})$$

is the surface Laplacian (or Laplace–Beltrami operator). Finally, we have that

$$\nabla^{(1)} \cdot \nabla^{(-1)} = -\xi S_\gamma^\alpha g^{\gamma\nu} \mathbf{t}_\alpha \cdot \frac{\partial \mathbf{n}}{\partial s_\nu} \frac{\partial}{\partial \xi} = -\xi S_\gamma^\alpha g^{\gamma\nu} K_{\alpha\nu} \frac{\partial}{\partial \xi} = -\xi S_\gamma^\alpha S_\alpha^\gamma \frac{\partial}{\partial \xi} = -\xi (\kappa_\alpha \kappa_\alpha) \frac{\partial}{\partial \xi}. \quad (\text{C.19})$$

The last equality is obtained by noticing that $S_\gamma^\alpha S_\alpha^\gamma$ is the trace of the square of the shape operator and thus $S_\gamma^\alpha S_\alpha^\gamma = \kappa_\alpha \kappa_\alpha$.

D Specialisation to plane-strain problems

The governing equations can be simplified in the case of plane-strain problems. We thus consider cylindrical geometries with arbitrary cross sections as shown in Fig. 9. We assume that the unit vectors \mathbf{e}_1 and \mathbf{e}_2 span the cross-sectional plane and that \mathbf{e}_3 is aligned with the axial direction. For clarity, we write $\mathbf{e}_3 \equiv \mathbf{e}_z$ and let $z \equiv x_3$ denote the axial coordinate. Using this construction, any vector \mathbf{u} can be decomposed into components \mathbf{u}_\parallel and u_z that lie in the cross-sectional plane and in the axial direction according to $\mathbf{u} = \mathbf{u}_\parallel + u_z \mathbf{e}_z$, with $\mathbf{u}_\parallel = u_\alpha \mathbf{e}_\alpha$.

In plane-strain problems, the deformation gradient tensor can be written as $\mathbf{F}(\mathbf{x}, t) = \mathbf{F}_\parallel(\mathbf{x}_\parallel, t) + \lambda_z \mathbf{e}_z \otimes \mathbf{E}_Z$, where $\mathbf{F}_\parallel = (\nabla_\parallel \mathbf{X}_\parallel)^{-1}$ is the in-plane deformation gradient tensor, $\mathbf{X}_\parallel = X_\alpha(\mathbf{x}_\parallel, t) \mathbf{E}_\alpha$, and $\lambda_z = (\partial X_z / \partial z)^{-1}$ corresponds to a constant stretch or compression that is imposed in the axial direction. The Jacobian can be decomposed as $J = J_\parallel \lambda_z$ where $J_\parallel = \det \mathbf{F}_\parallel$. We assume that all variables, except for X_z , are independent of the axial coordinate z .

The outer problem is trivial to formulate and will not be discussed in detail. Instead, we focus on the inner problem for the gel mechanics building upon the results from Sec. 3.2. The gel-bath interface can be parametrised in terms of $s_1 = s$ and $s_2 = z$ as $\mathbf{r}(s_1, s_2, t) = \mathbf{r}_\parallel(s, t) + z \mathbf{e}_z$. As illustrated in Fig. 9, the quantity \mathbf{r}_\parallel represents the one-dimensional gel-bath interface formed at each cross section, which is parametrised in terms of its arclength s . The corresponding unit

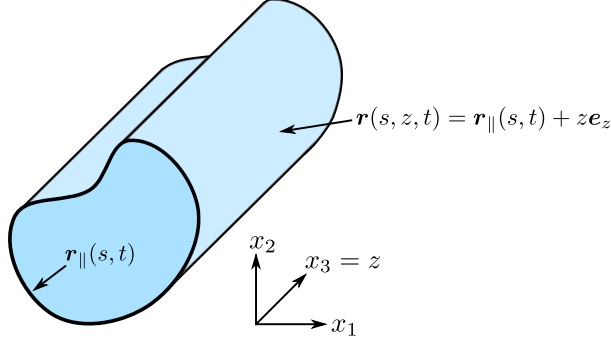


Figure 9: The geometry of a cylindrical hydrogel with arbitrary cross section. The quantity \mathbf{r}_{\parallel} represents the one-dimensional gel-bath interface formed at each cross section and it is parametrised by its arclength s . The full two-dimensional gel-bath interface \mathbf{r} is parametrised in terms of s and the axial coordinate z . The coordinates x_1 and x_2 lie in the cross-sectional plane.

tangent vectors are $\mathbf{t}_1 = \partial \mathbf{r}_{\parallel} / \partial s \equiv \mathbf{t}$ and $\mathbf{t}_2 = \mathbf{e}_z$ and satisfy $\mathbf{t} \cdot \mathbf{e}_z = 0$. The triad $\{\mathbf{t}, \mathbf{e}_z, \mathbf{n}\}$ thus forms an orthonormal basis. From the calculations in Appendix C, it follows that the principal curvatures of the surface are given by $\kappa_1 = -\mathbf{n} \cdot \partial_s \mathbf{t}$ and $\kappa_2 = 0$ and the derivatives in the inner region transform according to (3.12) with $\nabla_s = \mathbf{t} \partial_s + \mathbf{e}_z \partial_z$ and $\nabla_s^2 = \partial_{ss} + \partial_{zz}$.

To calculate the in-plane deformation gradient tensor in the inner layer, we again introduce the Lagrangian analogues of the gel-bath interface \mathbf{r}_{\parallel} , its arclength s , and the unit normal and tangent vectors \mathbf{n} and \mathbf{t} ; these are denoted by \mathbf{R}_{\parallel} , S , \mathbf{N} , and $\mathbf{T} = \partial_S \mathbf{R}_{\parallel}$, respectively. By repeating the calculations in Sec. 3.2, we find that the deformation gradient tensor is diagonal and given by

$$\tilde{\mathbf{F}}_{\parallel}^{(0)} = \left(\frac{\partial \tilde{\Xi}^{(0)}}{\partial \xi} \right)^{-1} \mathbf{n} \otimes \mathbf{N} + \lambda_s^{\text{gel}} \mathbf{t} \otimes \mathbf{T}, \quad (\text{D.1})$$

where $\lambda_s^{\text{gel}} = (\partial_s \tilde{S}^{(0)})^{-1}$ is analogous to the surface deformation gradient and quantifies stretching of material elements in the tangential direction. To calculate λ_s^{gel} , we match (D.1) to the outer solution and use the fact that \mathbf{t} and \mathbf{T} are unit vectors to obtain

$$\lambda_s^{\text{gel}} = \mathbf{t} \cdot \mathbf{F}^{\text{gel}} \cdot \mathbf{T}. \quad (\text{D.2})$$

The in-plane determinant is readily given by

$$\tilde{J}_{\parallel}^{(0)} = \left(\frac{\partial \tilde{\Xi}^{(0)}}{\partial \xi} \right)^{-1} \lambda_s^{\text{gel}}. \quad (\text{D.3})$$

while the in-plane components of the elastic stress tensor are

$$\tilde{\mathbf{T}}_{e,\parallel}^{(0)} = \frac{1}{\tilde{J}^{(0)}} \left(\tilde{\mathbf{B}}_{\parallel}^{(0)} - \mathbf{n} \otimes \mathbf{n} - \mathbf{t} \otimes \mathbf{t} \right), \quad (\text{D.4})$$

where $\tilde{\mathbf{B}}_{\parallel} = \tilde{\mathbf{F}}_{\parallel}^{(0)} (\tilde{\mathbf{F}}_{\parallel}^{(0)})^T$.

E Simplification of the equilibria for cylindrical gels

The nonlinear system for the outer solution (5.3) can be greatly simplified in the limit of a dilute salt, $\phi_+^{\text{bath}} \ll \phi_f$. Balancing terms in the electroneutrality condition (5.3c) gives

$$\Phi^{\text{gel}} - \Phi^{\text{bath}} \sim \log \left(\frac{z_f \phi_f}{\phi_+^{\text{bath}}} \right) + \mathcal{G} \left(\frac{1}{\lambda_z} - \frac{1}{J^{\text{gel}}} \right) + \frac{1}{J^{\text{gel}}} (1 - \chi \phi_s^{\text{gel}}), \quad (\text{E.1})$$

where we have assumed that $\mathcal{G}/J^{\text{gel}}$ at most $O(1)$ in size. The ion fractions in the gel are approximately given by

$$\phi_+^{\text{gel}} \sim \frac{(\phi_+^{\text{bath}})^2}{z_f \phi_f} \exp \left[-2\mathcal{G} \left(\frac{1}{\lambda_z} - \frac{1}{J^{\text{gel}}} \right) - \frac{2}{J^{\text{gel}}} (1 - \chi \phi_s^{\text{gel}}) \right], \quad \phi_-^{\text{gel}} \sim z_f \phi_f, \quad (\text{E.2})$$

showing that the anions, to leading order in ϕ_+^{bath} , balance the fixed charges on the polymer chains. Since the cation fraction ϕ_+^{gel} will be extremely small relative to the anion fraction ϕ_-^{gel} , the Jacobian determinant then reduces to

$$J^{\text{gel}} \sim \frac{1 + z_f \phi_f}{1 - \phi_s^{\text{gel}}}, \quad (\text{E.3})$$

where we have used $\phi_f = \varphi_f / J^{\text{gel}}$. The solvent fraction can then be obtained by solving

$$\log \phi_s^{\text{gel}} + \frac{1 - \phi_s^{\text{gel}}}{1 + z_f \phi_f} + \frac{\chi(1 - \phi_s^{\text{gel}})^2}{1 + z_f \phi_f} + \mathcal{G} \left(\frac{1}{\lambda_z} - \frac{1 - \phi_s^{\text{gel}}}{1 + z_f \phi_f} \right) = -2\phi_+^{\text{bath}}, \quad (\text{E.4})$$

and used to evaluate the Jacobian determinant, ion fractions, and jump in electric potential. The black dashed lines in Fig. 3 represent solutions of (E.3)-(E.4), which are in very good agreement with the full nonlinear system (5.3).

F The steady problem in cylindrical coordinates

In this section the full system of equations are specialised to a stationary axisymmetric situation in cylindrical coordinates. In this case, all of the fluxes and velocities are equal to zero and the chemical potentials are spatially uniform. As in Sec. 5, we consider a monovalent salt with $z_{\pm} = \pm 1$. The cylindrical hydrogel is assumed to be constrained in the axial direction such that the axial stretch is fixed to $\lambda_z = 1$.

F.1 The bath problem

In the far field ($r \rightarrow \infty$) we set $\Phi = 0$, $p = 0$, $\phi_+ = \phi_- = \phi_+^{\text{bath}}$. Since the chemical potentials are uniform, matching to the far field gives $\mu_{\pm} = \log \phi_{\pm} + \epsilon_r \beta^2 p \pm \Phi = \log \phi_+^{\text{bath}}$. The ionic volume fractions can therefore be expressed as

$$\phi_{\pm} = \phi_+^{\text{bath}} \exp(-\epsilon_r \beta^2 p \mp \Phi). \quad (\text{F.1})$$

Substituting (F.1) into the Poisson–Boltzmann equation for the potential (2.19) leads to

$$-\frac{\epsilon_r \beta^2}{r} \frac{d}{dr} \left(r \frac{d\Phi}{dr} \right) = -2\phi_+^{\text{bath}} \sinh(\Phi) \exp(-\epsilon_r \beta^2 p). \quad (\text{F.2})$$

The radial component of the stress balance (2.22) simplifies to

$$\frac{1}{r} \frac{d\Phi}{dr} \frac{d}{dr} \left(r \frac{d\Phi}{dr} \right) = \frac{dp}{dr}. \quad (\text{F.3})$$

These equations can be combined to determine the pressure:

$$p = \epsilon_r^{-1} \beta^{-2} \log \left(1 - 2\phi_+^{\text{bath}} (1 - \cosh \Phi) \right). \quad (\text{F.4})$$

The electric potential therefore satisfies the equation

$$\frac{\epsilon_r \beta^2}{r} \frac{d}{dr} \left(r \frac{d\Phi}{dr} \right) = \frac{2\phi_+^{\text{bath}} \sinh(\Phi)}{1 - 2\phi_+^{\text{bath}} (1 - \cosh \Phi)}. \quad (\text{F.5})$$

F.2 The gel problem

The chemical potentials in the gel can be written as

$$\log(1 - 2\phi_+^{\text{bath}}) = \Pi_s + \mathcal{G}p - \frac{\omega^2}{r} \frac{d}{dr} \left(r \frac{d\phi_s}{dr} \right), \quad (\text{F.6a})$$

$$\log \phi_+^{\text{bath}} = \Pi_{\pm} + \mathcal{G}p \pm \Phi, \quad (\text{F.6b})$$

where we have used the continuity of chemical potentials across the gel-bath interface (2.26). The osmotic pressures Π_m are defined in (2.10). The electric potential satisfies

$$-\frac{\beta^2}{r} \frac{d}{dr} \left(r \frac{d\Phi}{dr} \right) = \phi_+ - \phi_- + z_f \phi_f, \quad (\text{F.7})$$

with $\phi_f = C_f/J$. The deformation gradient tensor is written as

$$\mathbf{F} = \left(\frac{dR}{dr} \right)^{-1} \mathbf{e}_r \otimes \mathbf{e}_r + \frac{r}{R} \mathbf{e}_\theta \otimes \mathbf{e}_\theta + \mathbf{e}_z \otimes \mathbf{e}_z. \quad (\text{F.8})$$

The incompressibility condition simplifies to

$$R \frac{dR}{dr} = \frac{r}{J} = r(1 - \phi_s - \phi_+ - \phi_-). \quad (\text{F.9})$$

The radial and orthoradial elastic stresses are denoted as $T_{e,rr} = \mathbf{e}_r \cdot \mathbf{T}_e \cdot \mathbf{e}_r$ and $T_{e,\theta\theta} = \mathbf{e}_\theta \cdot \mathbf{T}_e \cdot \mathbf{e}_\theta$ and can be expressed as

$$T_{e,rr} = \frac{R}{r} \left(\left(\frac{dR}{dr} \right)^{-1} - \frac{dR}{dr} \right), \quad T_{e,\theta\theta} = \frac{dR}{dr} \left(\frac{r}{R} - \frac{R}{r} \right). \quad (\text{F.10})$$

The radial component of the stress balance (2.12) can be written as

$$\frac{dT_{e,rr}}{dr} + \frac{T_{e,rr} - T_{e,\theta\theta}}{r} + \omega^2 \mathcal{G}^{-1} \phi_s \frac{d}{dr} \left[\frac{1}{r} \frac{d}{dr} \left(r \frac{d\phi_s}{dr} \right) \right] + \frac{\beta^2 \mathcal{G}^{-1}}{r} \frac{d\Phi}{dr} \frac{d}{dr} \left(r \frac{d\Phi}{dr} \right) = \frac{dp}{dr} \quad (\text{F.11})$$

and can be simplified through the use of (F.6a) and (F.7) to

$$\frac{dT_{e,rr}}{dr} + \frac{T_{e,rr} - T_{e,\theta\theta}}{r} + \mathcal{G}^{-1} \phi_s \frac{d\Pi_s}{dr} - \mathcal{G}^{-1} (\phi_+ - \phi_- + \alpha_f J^{-1}) \frac{d\Phi}{dr} = (1 - \phi_s) \frac{dp}{dr}. \quad (\text{F.12})$$

F.3 Boundary conditions

At the origin of the hydrogel ($r = 0$) we impose

$$R = 0, \quad \frac{\partial \phi_s}{\partial r} = 0, \quad \frac{\partial \Phi}{\partial r} = 0. \quad (\text{F.13})$$

The first of these ensures that the Lagrangian origin is mapped to the Eulerian origin.

Due to the formulation of the model in terms of Eulerian coordinates, the deformed radius of the gel, a , is an unknown. Hence the steady problem is, in fact, a free boundary problem. The gel radius is implicitly defined by the equation $R(r = a) = 1$, where we have scaled the undeformed radius of the gel to one through a suitable non-dimensionalisation. At the gel-bath interface, continuity of electric potential and electric displacement leads to

$$\Phi|_{r=a^-} = \Phi|_{r=a^+}, \quad \frac{\partial \Phi}{\partial r} \Big|_{r=a^-} = \epsilon_r \frac{\partial \Phi}{\partial r} \Big|_{r=a^+}. \quad (\text{F.14})$$

In addition, the variational condition (2.27) becomes

$$\left. \frac{\partial \phi_s}{\partial r} \right|_{r=a^-} = 0. \quad (\text{F.15})$$

Continuity of stress at the free boundary implies that

$$\left[\mathcal{G}T_{e,rr} + \frac{\beta^2}{2} \left(\frac{\partial \Phi}{\partial r} \right)^2 + \phi_s (\Pi_s - \mu_s^{\text{bath}}) - \mathcal{G}(1 - \phi_s)p \right]_{r=a^-} = \epsilon_r \beta^2 \left[\frac{1}{2} \left(\frac{\partial \Phi}{\partial r} \right)^2 - p \right]_{r=a^+}, \quad (\text{F.16})$$

where $\mu_s^{\text{bath}} = \log(1 - \phi_+^{\text{bath}})$ and (F.6a) along with (F.15) have been used to simplify the Korteweg stress.

F.4 Numerical treatment

To numerically solve this problem, we use a Landau transformation and write $\hat{r} = r/a$. In addition, we rescale the Lagrangian radial coordinate as $\hat{R} = R/a$. The deformation gradient tensor is invariant under this transformation. However, the position of the free boundary is now explicitly determined by $\hat{R}(\hat{r} = 1) = 1/a$. The equations are discretised using finite differences and simultaneously solved using Newton's method with damping.

References

- [1] S.-k. Ahn, R. M. Kasi, S.-C. Kim, N. Sharma, and Y. Zhou. Stimuli-responsive polymer gels. *Soft Matter*, 4(6):1151–1157, 2008.
- [2] T. Bertrand, J. Peixinho, S. Mukhopadhyay, and C. W. MacMinn. Dynamics of swelling and drying in a spherical gel. *Physical Review Applied*, 6(6):064010, 2016.
- [3] G. L. Celora, M. G. Hennessy, A. Münch, B. Wagner, and S. L. Waters. The dynamics of a collapsing polyelectrolyte gel. *arXiv preprint 2105.06495*, 2021.
- [4] G. L. Celora, M. G. Hennessy, A. Münch, B. Wagner, and S. L. Waters. A kinetic model of a polyelectrolyte gel undergoing phase separation. *Journal of the Mechanics and Physics of Solids*, 2021.
- [5] M. S. Dimitriyev, Y.-W. Chang, P. M. Goldbart, and A. Fernández-Nieves. Swelling thermodynamics and phase transitions of polymer gels. *Nano Futures*, 3(4):042001, oct 2019.
- [6] L. Dong, A. K. Agarwal, D. J. Beebe, and H. Jiang. Adaptive liquid microlenses activated by stimuli-responsive hydrogels. *Nature*, 442(7102):551–554, 2006.
- [7] A. D. Drozdov and J. deClaville Christiansen. Modeling the effects of pH and ionic strength on swelling of polyelectrolyte gels. *The Journal of Chemical Physics*, 142(11):114904, 2015.
- [8] A. D. Drozdov, J. deClaville Christiansen, and C.-G. Sanporean. Inhomogeneous swelling of ph-responsive gels. *International Journal of Solids and Structures*, 87:11 – 25, 2016.
- [9] A. D. Drozdov, A. A. Papadimitriou, J. H. Liely, and C. G. Sanporean. Constitutive equations for the kinetics of swelling of hydrogels. *Mechanics of Materials*, 2016.
- [10] J. J. Feng and Y.-N. Young. Boundary conditions at a gel-fluid interface. *Physical Review Fluids*, 5(12):124304, 2020.

- [11] O. Gonzalez and A. M. Stuart. *A First Course in Continuum Mechanics*. Cambridge University Press, 2008.
- [12] W. Hong, X. Zhao, and Z. Suo. Large deformation and electrochemistry of polyelectrolyte gels. *Journal of the Mechanics and Physics of Solids*, 58(4):558–577, apr 2010.
- [13] F. Horkay, I. Tasaki, and P. J. Basser. Effect of monovalent-divalent cation exchange on the swelling of polyacrylate hydrogels in physiological salt solutions. *Biomacromolecules*, 2(1):195–199, 2001.
- [14] J. Hua, M. K. Mitra, and M. Muthukumar. Theory of volume transition in polyelectrolyte gels with charge regularization. *The Journal of Chemical Physics*, 136(13):134901, 2012.
- [15] D. Komoto, T. Furuike, and H. Tamura. Preparation of polyelectrolyte complex gel of sodium alginate with chitosan using basic solution of chitosan. *International Journal of Biological Macromolecules*, 126:54 – 59, 2019.
- [16] E. Y. Kramarenko and A. R. Khokhlov. Intranetwork phase separation in polyelectrolyte gels. *Polymer Gels and Networks*, 6(1):45 – 56, 1998.
- [17] H. J. Kwon, Y. Osada, and J. P. Gong. Polyelectrolyte gels-fundamentals and applications. *Polymer Journal*, 38(12):1211–1219, 2006.
- [18] J. Li and D. Mooney. Designing hydrogels for controlled drug delivery. *Nature Reviews Materials*, 1:16071, 2016.
- [19] Y. Mori, H. Chen, C. Micek, and M.-C. Calderer. A dynamic model of polyelectrolyte gels. *SIAM Journal on Applied Mathematics*, 73(1):104–133, 2013.
- [20] M. Mussel and F. Horkay. Experimental evidence for universal behavior of ion-induced volume phase transition in sodium polyacrylate gels. *Journal of Physical Chemistry Letters*, 10(24):7831–7835, 2019.
- [21] I. Ohmine and T. Tanaka. Salt effects on the phase transition of ionic gels. *The Journal of Chemical Physics*, 77(11):5725–5729, 1982.
- [22] T. K. Sherwood, R. L. Pigford, and C. R. Wilke. *Mass Transfer*. McGraw-Hill Book Co, New York, 1975.
- [23] A. Sidorenko, T. Krupenkin, A. Taylor, P. Fratzl, and J. Aizenberg. Reversible switching of hydrogel-actuated nanostructures into complex micropatterns. *Science*, 315(5811):487–490, 2007.
- [24] R. W. Style, T. Sai, N. Fanelli, M. Ijavi, K. Smith-Mannschott, Q. Xu, L. A. Wilen, and E. R. Dufresne. Liquid-liquid phase separation in an elastic network. *Physical Review X*, 8(1):011028, 2018.
- [25] X. Wang, W. Hong, et al. Surface interactions between two like-charged polyelectrolyte gels. *Physical Review E*, 81(4):041803, 2010.
- [26] K.-A. Wu, P. K. Jha, and M. O. de la Cruz. Control of nanophases in polyelectrolyte gels by salt addition. *Macromolecules*, 43(21):9160–9167, 2010.
- [27] K.-A. Wu, P. K. Jha, and M. Olvera de la Cruz. Pattern selection in polyelectrolyte gels by nonlinear elasticity. *Macromolecules*, 45(16):6652–6657, 2012.

- [28] T. Yamamoto and M. Doi. Electrochemical mechanism of ion current rectification of polyelectrolyte gel diodes. *Nat. Commun.*, 5:4162, 2014.
- [29] E. Yariv. An asymptotic derivation of the thin-Debye-layer limit for electrokinetic phenomena. *Chemical Engineering Communications*, 197(1):3–17, 2009.
- [30] Y. Yu, C. M. Landis, and R. Huang. Salt-induced swelling and volume phase transition of polyelectrolyte gels. *Journal of Applied Mechanics*, 84(5):051005, 2017.
- [31] H. Zhang, M. Deghany, and Y. Hu. Kinetics of polyelectrolyte gels. *Journal of Applied Mechanics*, 87(6), 2020.